Powering Biomedical Devices

Powering Biomedical Devices

Edwar Romero

ELSEVIER

AMSTERDAM • BOSTON • HEIDELBERG • LONDON
NEW YORK • OXFORD • PARIS • SAN DIEGO
SAN FRANCISCO • SINGAPORE • SYDNEY • TOKYO
Academic Press is an imprint of Elsevier

Academic Press is an imprint of Elsevier
The Boulevard, Langford Lane, Kidlington, Oxford, OX5 1GB, UK
225 Wyman Street, Waltham, MA 02451, USA

First published 2013

Notices
Knowledge and best practice in this field are constantly changing. As new research and experience broaden our understanding, changes in research methods, professional practices, or medical treatment may become necessary.

Practitioners and researchers must always rely on their own experience and knowledge in evaluating and using any information, methods, compounds, or experiments described herein. In using such information or methods they should be mindful of their own safety and the safety of others, including parties for whom they have a professional responsibility.

To the fullest extent of the law, neither the Publisher nor the authors, contributors, or editors, assume any liability for any injury and/or damage to persons or property as a matter of products liability, negligence or otherwise, or from any use or operation of any methods, products, instructions, or ideas contained in the material herein.

British Library Cataloguing in Publication Data
A catalogue record for this book is available from the British Library

Library of Congress Cataloging-in-Publication Data
A catalog record for this book is available from the Library of Congress

ISBN: 978-0-12-407783-6

PREFACE

Biomedical technology has evolved through the decades for specialized medical care and treatment of a number of conditions and we expect it to continue evolving. For instance, the first cardiac pacemaker in the 1960s, using the now discontinued mercury-oxide cell, provided 2–3 years of operation. Nowadays, pacemakers can operate reliably for 10 years. The lithium-based battery technology used by the 1970s helped to propel that feat. We also expect biomedical technology to merge with electronic devices for noninvasive and implantable devices for health care. Due to the surge in wireless communications, and partly because of the ease of connection without the need for wires, we are also expecting this venue to permeate a number of applications, such as for health-care monitoring. Although there are a number of concerns regarding privacy, there are technical details about the transmission of information by itself. However, what about the batteries?

Being an engineer doing research on energy harvesting I wondered if there are technologies that makes it possible to harness energy from the surroundings to power our gadgets. If there are mechanical and electromechanical self-winding wristwatches, what about low-power monitoring devices for health purposes? Before that, I always had in my mind other questions in order to see this idea become a possibility. How much energy is available? Is there a limit for generation? What can be powered with it? I only found partial answers to these questions. Thus, the purpose of this book is to answer most of the questions I had in my mind for a number of years.

I expect the book's structure gives you an idea of the future possibilities for energy harvesting in biomedical applications. The Introduction discusses the challenges in the near future for health care while at the same time explaining about technology trends, energy harvesting, and the overall limits of the energy generating technology at small scale. Power Sources talks over the actual power sources, battery technology, the power available from the human body, and the power limits for kinetic energy generators while applying this approach to walking and running. Enabling Technologies describes the different approaches to

generate energy from the human body, with special emphasis in kinetic energy generators reported in the literature. Power Consumption and Applications reports actual medical devices (especially implantable medical devices), the applications and power consumption to have an idea of what could be powered with energy harvesters. Future Trends considers the challenges and possibilities for this technology to be employed in the near future. It is my personal expectation to have provided the tools and foundation for designing and deciding about alternative powering options for biomedical devices.

I would like first to acknowledge the vast array of researchers on whose work this book came to be. I hope to have honored you. On a personal level, I also would like to thank Prof. Robert Warrington to encourage me to try and to keep going forward. There are things you don't fully appreciated until later on. I would like to show my appreciation to Prof. Michael Neuman to inspire me into looking for different directions, even in different disciplines; I think I never congratulated him for it. I know I learned lessons for life from both of you. Finally, I wish to thank my wife for supporting me this time.

I would also like to express my appreciation to Joe Hayton, Chelsea Johnston, Lisa Jones and all the staff at Elsevier for their quality production of the book.

CHAPTER 1

Introduction

The increase of world population is a challenge itself for world resources. The sustainability of food supplies, energy resources, and the environment are being questioned by analysts, while climate change just adds more pressure to the equation. The life expectancy of the world as a whole is rising while the fertility rate is declining. This will create a challenge in health care for the ageing population (Gavrilov and Heuveline, 2003). The United States alone will have 20% of the population over the age of 65 by 2050. In contrast, Europe will see rates close to 30% while Japan will arise to almost 40%, as summarized in Table 1.1. It is anticipated that in the near future, specialized health-care services will be in higher demand due to this increase. This demand will be characterized by medical resources not only to attend to this segment of the population, but also to keep them active as well. Therefore, the monitoring of physiological responses as well as specialized drug or other therapy delivery applications will be needed for portable, wearable, or implantable biomedical autonomous devices. In addition, wireless communication promises new medical applications such as the use of wireless body sensor networks for health monitoring (Jovanov et al., 2005; Hao and Foster, 2008; Varshney, 2007).

These biomedical devices, however, come with their own issues, mainly power source challenges. Batteries are commonly used to energize most of these applications, but they have a finite lifetime. As biomedical

Table 1.1 Percentage of Population Over 65 Years Old[a]

Region	1950	2000	2050
World	5.2	6.8	16.2
USA	8.3	12.4	21.6
Europe	8.2	14.8	27.4
Japan	4.9	17.2	37.8

[a]*Population Division of the Department of Economic and Social Affairs of the United Nations Secretariat, World Population Prospects: The 2008 Revision, http://esa.un.org/unpp.*

devices tend to be relatively power hungry, a trade-off between battery capacity and size has governed the lifespan, dimensions, and capabilities for battery-powered devices. New technologies such as energy harvesting have the capability to effectively power electronic instruments. Harnessing energy from sources such as motion, sunlight, and temperature changes has been employed respectively on electronic self-winding wristwatches, solar-powered calculators, and thermal-powered wristwatches. Therefore, energy harvesting is an alternative to batteries for energizing electronic devices.

Energy harvesting was the main technology used before the advent of the internal combustion engine, the power grid, or batteries. For instance, wind turbine farms and hydroelectric plants are the successors of windmills and water wheels. Small electrical generators were also used in radios and flashlights operated by hand cranking in the 1940s. Other recent examples include the bicycle dynamo (capable of producing up to 3 W of power) and lever-driven mobile phone chargers (up to 2 W of power) (Flipsen, 2006; van Donk, 2000). Industrial applications for recent vibration energy harvesters have been developed to power autonomous wireless sensor nodes (Ferro Solutions, Inc.[1], Perpetuum Ltd.[2]). Energy scavenging of water flow in oceans and rivers are exploited as well (Taylor et al., 2001) (similar to an eel swimming, one device uses the traveling vortices in water to strain piezoelectric polymers). One of the most well-known examples of energy harvesting from body motion is the self-winding wristwatch mechanism that evolved from being entirely mechanical (wind-up) to use a hybrid approach (using a miniature electromagnetic generator to charge a battery).

Wearable microinstruments for environmental monitoring of humidity, temperature, pressure, and acceleration with data processing capabilities have been successfully implemented as watch-sized devices (Mason et al., 1998; Najafi, 2000; Yazdi et al., 2000). Such systems are commonly powered by batteries, and sometimes the battery is larger than the entire system. This is normally the case for devices that need to be functional for long periods of time. For example, batteries for cardiac pacemakers occupy half the device's volume (Mallela et al., 2004), while their average lifetime is between 5 and 12 years (Katz and Akiyama, 2007). Implantable biomedical devices, such as neural

[1] http://www.ferrosi.com.
[2] http://www.perpetuum.com.

prostheses (Gage et al., 2005; Johnson et al., 2004; Oweiss et al., 2005), are also dependent on microsystems for their operation. The use of radio frequency (RF) induction for power and radio telemetry is the best alternative when wires or batteries are not an option, which is the case for some integrated neural stimulation microsystems (Najafi, 2000). This approach uses an external flat antenna and an implanted on-chip antenna. These types of microsystems could also benefit from energy harvesting to avoid battery limitations. To address the need for more efficient technology, researchers have tried to employ energy harvesters for powering biomedical devices, as evidenced by investigations of automatic self-winding wristwatches for powering pacemakers (Gorge et al., 2001; Goto et al., 1998, 1999) or by using generators placed in shoes for powering artificial organs (Antaki et al., 1995).

The decrease in power consumption by electronic devices has been well documented over the years. A custom digital signal processing (DSP) unit consumed about 18 μW of power by 1998 (Amirtharajah and Chandrakasan, 1998). An updated version from the same group presented a power consumption of 500 nW by 2005 (Amirtharajah et al., 2005), while another group in 2008 presented a processor called Phoenix using only 30 pW of power (Seok et al.; 2008). Therefore, low-power electronics are making progress to extend battery life or even use energy harvesting as the sole energy source. If electronic self-winding wristwatches can harness body motion to power themselves, in the near future hybrid approaches using energy harvesters and rechargeable batteries could power more portable applications or even implantable devices. It is anticipated that hybrid power supplies will be critical for a wide range of autonomous microsystems (Bharatula et al., 2005; Harb et al., 2002).

Another concern is the environmental panorama of battery disposal around the world. Millions of batteries are discarded into sanitary landfills where heavy metals can result in groundwater contamination. Therefore, solutions that minimize or avoid battery disposal will certainly provide an environmental advantage.

Power consumption is intrinsically attached to the device's operation. In addition, the larger the device, the larger the power consumption. Cardiac pacemakers consume around 100 μW of electrical power in average, while hearing aids, on the other hand, require around 50 μW of power. The latter, although consuming less power, involve frequent

battery replacement (Flipsen et al., 2004). Implantable neurostimulators and infusion pumps have larger power consumption and have longevity of 3–5 years (Paulo and Gaspar, 2010). Longer battery lifespan is always desired because it reduces medical care costs for surgically implantable devices. It also makes it possible to add more functionality or more frequent measurement of physiological parameters for a given battery duration.

1.1 TECHNOLOGY TREND

Computer technology has progressed aggressively over the last two decades as shown in Figure 1.1, but it is also clear that battery technology has not kept the same pace. This energy source, although increased in capacity over the years, seems to slow down the progress for portable electronics to gain a wider adoption. It is evident that advances in computational capabilities outpace the battery development; hence, more applications could be envisioned if batteries followed the trend of computer technology. For instance, the cost of battery replacement prohibits a wider deployment of wireless sensor networks. As a result, other energy sources are needed to cover the increasing demands of new electronic applications. Energy harvesting can be an option to solve this problem.

Figure 1.1 represents the increase in performance for several technologies compared against those available in 1990; for instance, disk capacity increased by a factor of 10,000 between 1990 and 2010 while

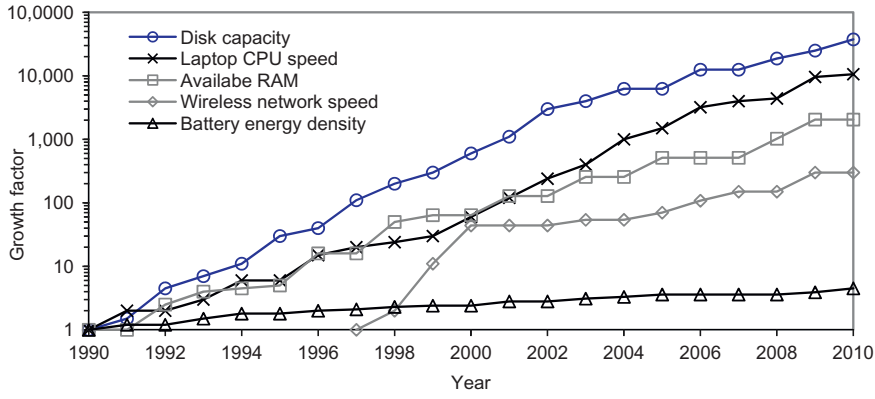

Figure 1.1 Electronics trend since 1990 (Romero, 2010; Starner and Paradiso, 2004).

battery energy density increased only 5×. This graph is an extension of the one presented by Starner and Paradiso (2004) that covered the period from 1990 to 2003. The reference point for the comparisons was kept the same: a high-end portable computer from 1990, with an 80386 processor running at 16 MHz, 8 MB of RAM and 40 MB of hard disk capacity, using a nickel–cadmium battery. The latest technologies were compared for each year as multiples of the reference laptop. Only disk capacity and available RAM data were kept from Starner and Paradiso from the years 1990 to 2003. Specialized computer magazines over the Internet were used to obtain most of the information. As there are several central processing unit (CPU) benchmarking comparisons, the number of million instructions per second (MIPS) for Intel processors was used as a reference providing a similar trend line as the one from the work of Starner and Paradiso. The battery energy density was based on the volumetric energy density (Wh/L) data gathered from Panasonic[3] for nickel–cadmium, nickel–metal hydride, and lithium–ion battery chemistries, because it was readily available until 2010. Although Starner and Paradiso calculated the energy density using joules per kilogram, the results are nearly identical. The IEEE 802.11 standard released in 1997 was included for the wireless network speed trend.

On the other hand, energy sources other than batteries exist with even higher power densities, as shown in Figure 1.2, but most of them are designed for macroscale systems and/or require a combustible to operate. The human body is also an alternative energy source that can provide power densities under 1 W/kg (1 mW/g) or 1 W/L (1 mW/cm^3) as shown in the figure. Due to the decrease in power consumption of electronic devices mentioned previously, the available power density levels of 1 mW/cm^3 or 1 mW/g are an interesting option for low-power applications. Because the power is generated by body motion, the applications that can directly benefit for this approach are portable electronics and biomedical devices (wearable or surgically implantable).

Figure 1.3 highlights the power budget for some electronic applications within the human body generation range. For example, using the previous reference of 1 mW/cm^3 (or 1 mW of power in a volume of 1 cm^3) only a few miniature low-power applications (such as pacemakers, hearing aids, watches, and some consumer devices) can directly

[3]http://www.panasonic.com.

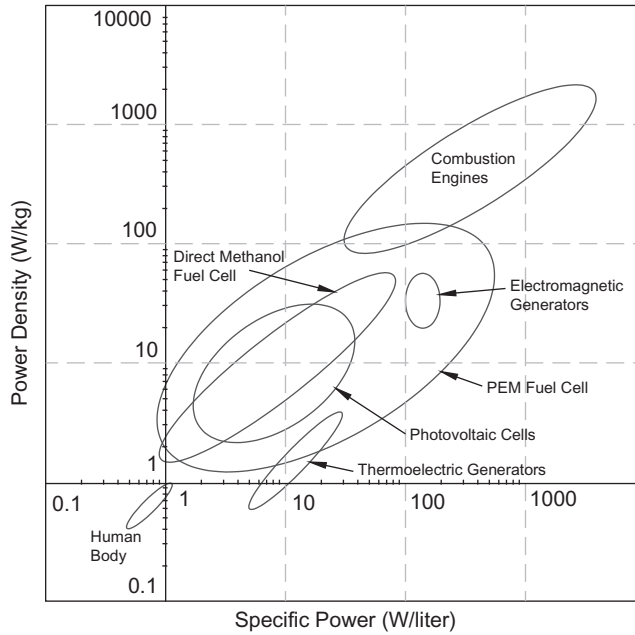

Figure 1.2 Comparison of power sources. Chart adapted from Flipsen (2006).

use the energy harvesting approach. However, larger generator volumes can produce higher power outputs. Continuing with the reference of 1 mW/cm^3, a relatively small generator with a volume of 10 cm^3 could produce up to 10 mW. According to the chart in Figure 1.3, 10 mW can be used to power some remote controls and communication devices (pagers). Taking as a reference the shoe generator presented by Kymissis et al. (1998) with a power generation over 200 mW, some radios and cell phones can be powered by energy harvesting.

Figure 1.3 describes the power requirements of several electronic products ranging from medical devices to consumer products (power consumption from 1 μW up to several watts). This figure also includes the power output of one energy harvester (a shoe generator) and several human-operated generators for comparison purposes. Although human-operated generators have a power output enough to energize power-hungry devices (such as notebook computers), they require active generation.

On the other hand, passive generation, although producing a lower power output, produces an adequate amount to energize low-power electronic applications, including some medical devices. Therefore, it is

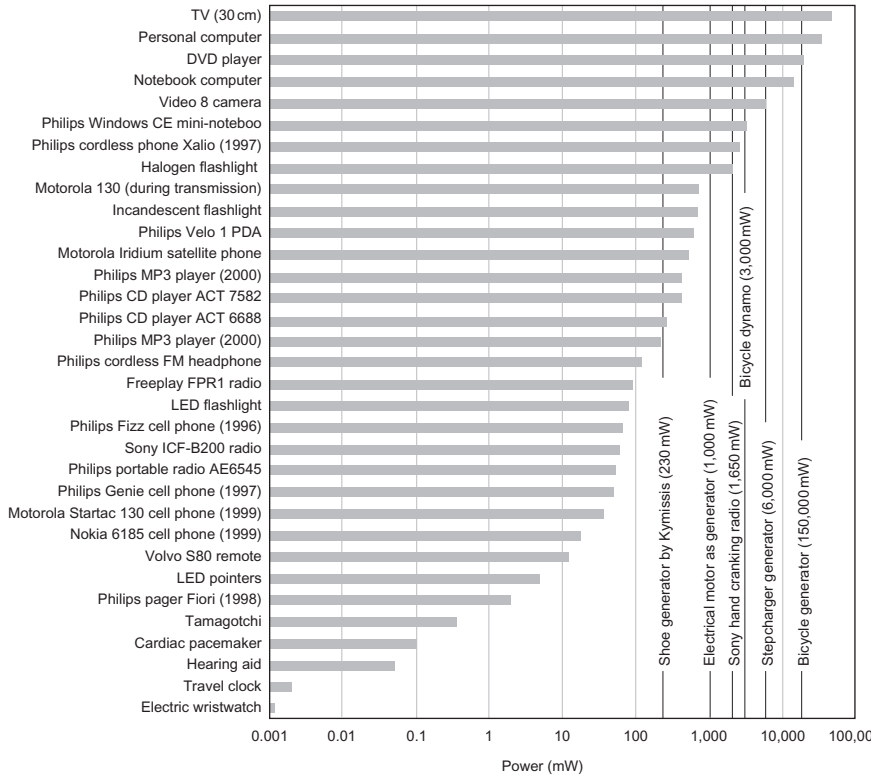

Figure 1.3 Comparison of power consumption (horizontal bars) against power generation (vertical lines) for some electronic devices. Chart adapted from Flipsen (2005).

clear that energy harvesting from body motion has the potential to power some biomedical applications and other low-power devices.

1.2 ENERGY HARVESTING

Energy harvesting is the process in which energy is produced from external sources, such as air or water flow, vibrations or motion, solar energy, or thermal gradients. The term is usually applied to power generation for small, portable, wearable, or autonomous devices. In recent times, energy harvesting is a research area that is gaining relevance for powering electronic devices because of the almost infinite lifetime potential. Energy generation from motion, solar light, and temperature changes has proven to be a viable alternative to batteries for commercial products, such as hand-cranking radios and flashlights, solar-powered calculators, and thermal-powered wristwatches. Energy scavenging also

addresses the feasibility of using body motion to power portable, wearable, or implantable systems, such as biomedical applications.

Kinetic or inertial energy harvesting uses external vibration or motion to generate energy. This external vibration can be in the form of engine or machine-based vibrations (constant frequency vibrations), while motion can be associated with human activities, environment movement, or oscillations with low-frequency, large amplitude, and broad-frequency spectra. Energy scavenging from kinetic generators uses the external vibration or motion to produce electricity. The kinetic energy is transferred to a proof mass where several transduction techniques can be employed to transform it to electrical energy. These devices are typically designed to match their natural resonant frequency with that of the energy source to maximize their power output. Linear-based energy harvesters are found to be well suited for machine vibrations because mechanical vibrations are relatively uniform (constant frequency) with a main vibration axis.

Mechanical vibration has an energetic content in the form of kinetic energy. A better estimation of the available energy leads to a better match of energy harvesters for a given external source. One of the questions that need to be solved is how much energy is available in order to determine how it can be harvested. In order to solve that question, the transduction generation (how to transform one form of energy into another) needs to be analyzed to determine if there are generation limits. Kinetic energy harvesting is studied later to define the parameters that need to be considered for this evaluation.

On the other hand, the increasing use miniature low-power electronics and wireless technologies for new medical monitoring applications, such as body sensor networks for health monitoring (Hao and Foster, 2008; Jovanov et al., 2005; Varshney, 2007), will challenge present technologies due to battery finite lifetime and size. A trade-off between battery size and battery capacity has typically dominated the final size, lifetime, and capabilities of a system.

The scavenging of body motion for powering portable mechanical devices was first reported in 1770 when the Swiss watchmaker Abraham Louis Perrelet[4] invented the self-winding mechanism for

[4]http://www.hautehorlogerie.org/en/history/watchmakers/XVIII/abraham-louis-perrelet-28/. Retrieved January 29 2013.

pocket watches The mechanism was designed to wind the watch's mainspring as the person walked. This was achieved using an oscillating weight inside the watch mechanism. By 1924, John Harwood adapted a similar mechanism for wristwatches (Day and McNeil, 1995). His design allowed the mainspring to wind only when the weight oscillated in one direction. Because spring bumpers limited the swinging to less than 360°, this design is now known as a bumper wristwatch. By the 1960s, self-winding wristwatches without spring bumpers, for full rotations, became common, but it wasn't until 1986[5] when the Japanese company Seiko made an updated version that included a tiny electrical generator.

Energy harvesting makes use of several transduction techniques to produce energy. Generation due to physical motion commonly involves the use of electromagnetic induction, piezoelectric generation, or electrostatic transduction. Other practical methods include the use of thermal gradients, photovoltaic cells, or a combination of the above techniques. A brief description is given for each of these.

Electromagnetic generation is based on the induced voltage in a coil when a magnet moves relative to it. This is produced by the changing magnetic flux as described by the Faraday's law of induction

$$|E| = |d\phi_B/dt| \tag{1.1}$$

where $|E|$ is the magnitude of the electromotive force (EMF) in volts and ϕ_B is the magnetic flux in webers. This change is due to having a fixed magnet and a moving coil or the opposite, a fixed coil and a moving magnet. For a coil, the EMF depends on the number of coil turns, the strength of the magnetic flux, and the rate of change of the magnetic flux. A typical architecture might be a magnet attached to a cantilever beam (similar to a small diving board), or spring that oscillates with respect to a coil, or a free sliding magnet within a helical coil that surrounds the magnet.

Piezoelectric transduction for energy harvesting is based on the voltage produced when a piezoelectric material is subject to mechanical deformation. The amount of voltage produced is dependent on the properties of the material, the amount of deformation, and the direction

[5]http://www.seikowatches.com/baselworld/2007/press/details/070412_07.html. Retrieved January 29 2013.

of the applied forces. A common arrangement for piezoelectric generators is the cantilever beam architecture. The cantilever beam is either subject to mechanical deformation or subject to an external vibration. The cantilever beam is typically designed with the objective to match its natural resonant frequency to that of the external vibration.

Energy generation from electrostatic transduction is based on the charging of capacitor plates. The separation of charged capacitor plates is varied by environmental motion or vibration and changing the capacitance of the capacitor structure. The change in capacitance changes the voltage across the capacitor according to the fundamental capacitor relationship:

$$Q = CV \tag{1.2}$$

where the charge on the capacitor Q is equal to the capacitance C times the voltage V. When the capacitance is decreased (by an increasing separation of the capacitor plates), the voltage through the capacitor increases (because there is a charge on the capacitor). Therefore, the mechanical energy due to vibrations or motion that increases the plate separation is converted into electrical energy.

1.3 ENERGY LIMITS

Transduction generation limits are defined as energy per volume, or energy density, and expressed with the lower case letter u. Maluf and Williams (2004) offered one of the first descriptions for the transduction limits for thermal, electromagnetic, piezoelectric, and electrostatic generation. The thermal approach is based on the thermal expansion u_{te} (for one dimension) defined as

$$u_{te} = \frac{1}{2} Y(\alpha \Delta T)^2 \tag{1.3}$$

where Y is the Young's modulus, α is the coefficient of thermal expansion (the volumetric thermal expansion is approximately 3α), and ΔT is the temperature difference. Different materials will have different energy densities based on their properties, this is shown in Figure 1.4A. This energy density can reach values near 400 mJ/cm^3 depending on the material considered for a temperature difference of 25°C. A temperature difference between 37°C from the human body and 22°C environment leads to 15°C gradient. This gradient still

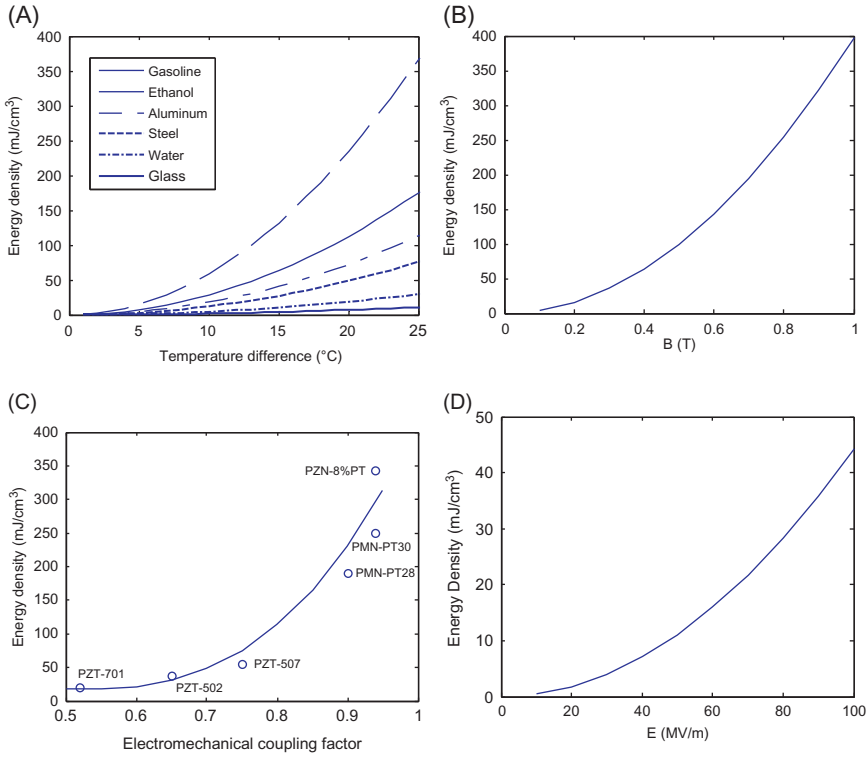

Figure 1.4 Transduction generation limits: (A) thermal expansion, (B) electromagnetic, (C) piezoelectric, and (D) electrostatic (Romero, 2010).

provides energy densities of tens of milliwatt per cubic centimeter. However, the requirement of a thermal gradient limits where such a generator can be placed. Generators placed against the skin use the difference in temperature between the body and the surrounding environment. Inside the human body such a generator would be severely limited as it is estimated that gradients will never exceed 0.2°C (Luchakov and Nozdrachev, 2009). In addition, harvesting the thermal expansion of a material for energy generation is not a simple task.

Thermoelectric energy conversion makes use of a temperature gradient to create an electric potential for thermoelectric materials. The Carnot efficiency η_c

$$\eta_c = (T_{\text{high}} - T_{\text{low}})/T_{\text{high}} \tag{1.4}$$

provides a limit for this generation (where T stands for temperature). If body temperature (37°C) and a cool room (25°C) are considered, the

efficiency of the generation is only 5.5%. Yet, commercial thermoelectric generators are able to produce 60 $\mu W/cm^2$ for a temperature gradient of 5°C from body heat waste (Paradiso and Starner, 2005).

The energy density for an electromagnetic generator (Maluf and Williams, 2004) is defined as

$$u_{em} = \frac{1}{2} B^2/\mu_0 \tag{1.5}$$

where B is the magnetic field and μ_0 is the permeability of free space ($\mu_0 = 4\pi \times 0^{-7}$ H/m). Assuming a maximum value of 1 T for the magnetic flux B yields to a maximum theoretical of 400 mJ/cm^3, as shown in Figure 1.4B. A modest value of 0.1 T has an energy density of 4 mJ/cm^3, which can be considered as a practical obtainable value.

The maximum energy density for a piezoelectric material (Roundy and Wright, 2004) is given as

$$u_{pe} = 1/(2Y)\sigma_y^2 k^2 \tag{1.6}$$

where σ_y is the yield strength of the material, k is the electromechanical coupling coefficient, and Y is the modulus of elasticity. The previous expression can also be presented as

$$u_{pe} = 1/(2\varepsilon)\sigma_y^2 d^2 \tag{1.7}$$

where d is the piezoelectric charge constant and ε is the permittivity or dielectric constant. Using the properties of a high performance piezoelectric material, such as the single crystal PZN-8%PT ($Pb(Zn_{1/3}Nb_{2/3})O_3$-$PbTiO_3$, Ritter et al., 2000), the theoretical maximum value is 343 mJ/cm^3. Employing the properties of a common piezoelectric material, such as PZT-5H ($Pb(Zr,Ti)O_3$, PZT-501 from Morgan Electro Ceramics plc) with a safety factor of 2, an energy density of 19 mJ/cm^3 can be considered as a practical value. The trend for the piezoelectric materials of Table 1.2 is shown in Figure 1.4C.

The energy density for electrostatic generation (Maluf and Williams, 2000), such as a capacitor, is defined as

$$u_{es} = \frac{1}{2} \varepsilon E^2 \tag{1.8}$$

where ε is the dielectric constant and E is the electric field. Using the permittivity of the free space ($\varepsilon_0 \approx 8.85 \times 10^{-12} A^2 s^4/(kg\ m^3)$) and a

Table 1.2 Piezoelectric Material Properties

Material	Y (GPa)	σ_y (MPa)	d_{33} (pm/V)	k_{33} (CV/Nm)	$\varepsilon/\varepsilon_0$
PZT-701[a]	90	80	153	0.52	425
PZT-501[a]	62	80	450	0.65	1950
PZT-507[a]	62	80	820	0.75	4400
PMN-PT28[a]	300	80	1700	0.90	5500
PMN-PT30[a]	210	80	2200	0.94	7000
PZN-8%PT[b]	8.3	80	2200	0.94	5100

[a] *Morgan Electro Ceramics plc.*
[b] *Ritter et al. (2000)*

maximum electric field of 100 MV/m (or a field of 100 V over 1 μm) gives a theoretical maximum value of 44 mJ/cm^3, as shown in Figure 1.4D. A modest E of 30 MV/m produces 4 mJ/cm^3, which can be considered as a practical value.

In summary, assuming a frequency of 1 Hz (similar to human walking, about one cycle per second), power (energy/time) calculations for the electromagnetic transduction is limited to a maximum theoretical value of 400 mW/cm^3 (4 mW/cm^3 practical value), piezoelectric generation can be as high as 343 mW/cm^3 (19 mW/cm^3 practical), while electrostatic transduction is limited to 44 mW/cm^3 (4 mW/cm^3 practical), see Table 1.2. These findings were also presented earlier by Roundy (2003) in terms of energy as millijoules per cubic centimeter.

The transduction technology does not limit how much energy can be harvested since over 1 mW of power can be produced by walking from a 1 cm^3 generator (according to Table 1.2). Therefore, the next question to answer is: How much energy is actually available and how much can be scavenged?

CHAPTER 2

Power Sources

2.1 ACTUAL POWER SOURCES

As most devices are being powered by batteries, Table 2.1 presents the energy content of several sources to keep them in perspective. It is interesting to see the energy content of 1 L of gasoline is comparable in order of magnitude as the average daily calorie intake. Combustion engines are without doubt the kings because they provide energy at several orders of magnitude over batteries. Although actual technology has evolved at a fast pace, battery technology is still lagging behind, but nanotechnology promises new developments.

Zinc/mercuric oxide batteries were the first type of battery used for the first cardiac pacemaker implanted in 1960, but they lasted between 2 and 3 years (zinc/mercuric oxide or mercury cells are no longer manufactured because of the mercury content). However, it wasn't until the use of lithium batteries in the 1970s that equipment with longevity over 10 years was a possibility (Holmes, 2001). After successful implementation of the pacemaker, similar techniques were employed to treat other conditions. Implanted defibrillators and neurostimulators took advantage of this. While pacemakers are low current drain devices, neurostimulators operate with medium rate currents (1−5 mA) and defibrillators with high pulse power (Drews et al., 2001). Implantable biomedical devices are powered by batteries or by inductive links. Inductive link is radio frequency using coupling coils where an implanted coil receives power and communication when coupled with an external coil. As

Table 2.1 Summary of Energy Sources

Source	Energy (J)
Button cell battery	$\sim 10^3$
AA battery, cellphone battery	$\sim 10^4$
Laptop battery	$\sim 10^5$
Lead acid battery	$\sim 10^6$
Liter of gasoline	$\sim 10^7$
Average human diet (per day)	$\sim 10^7$

batteries are the most common approach, they are discussed in terms of capacity and service life.

Battery capacity is usually expressed in terms of energy in Joules (J) or more commonly in watt-hours (Wh). Power is the rate of energy use (energy/time, where time is expressed in seconds), watt-hours or more commonly kilowatt-hours (kWh, 1,000 Wh = 1 kW) is a unit of energy (for instance, 10 h of regular use of a home appliance rated at 1,500 W will consume 15,000 Wh or 1.5 kWh). Batteries are also rated for specific energy (energy/mass or Wh/kg) or energy density (energy/volume or Wh/L), the amount of energy available per mass or per volume depending on the intended application. Table 2.2 summarizes the battery ratings of primary cells (disposable batteries), while Table 2.3 summarizes the ratings for secondary cells (rechargeable batteries). The nominal voltage depends exclusively on the chemical reactions of its components. Common types of batteries are the zinc–carbon and alkaline (sizes AAA, AA, C, D, 9V), as well as zinc–air and

Table 2.2 Ratings of Primary Cells (Disposable Batteries)

Battery Type	Specific Energy (Wh/kg)	Energy Density (Wh/L)	Nominal Voltage (V)	Service Life
Zinc–carbon (Zn/C)	36	60–120	1.5	2 years
Alkaline (zinc–manganese dioxide, Zn/MnO_2)	110–210	320	1.5	7 years
Zinc–air (Zn–air)	470	1480	1.35–1.65	3 years shelf life; 3–12 weeks use
Silver-oxide (silver–zinc)	130	500	1.55	5 years
Lithium (lithium–manganese dioxide, $LiMnO_2$)	330	550–650	2.8	5 years
Lithium (lithium-thionyl chloride, $LiSOCl_2$)	760	800–1420	3.6	10–20 years
Lithium (lithium–iodine, $Li–I_2$)	150–250	900	2.8	10 years
Lithium (lithium–silver–vanadium oxide, $Li–Ag_2V_4O_{11}$, Li–SVO)	150	410	2.75	6 years

Adams (1995)
Drews et al. (2001)
Chen et al. (2006)
http://www.saftbatteries.com
http://machinedesign.com/artice/lithium-battery-basics-0306
http://www.energizer.com
http://www.duracell.in/en-IN/power-education/alkaline-benefits.jspx
http://www.allaboutbatteries.com/Battery-Energy.html

Table 2.3 Ratings of Secondary Cells (Rechargeable Batteries)				
Battery Type[a,b,c]	**Specific Energy (Wh/kg)**	**Energy Density (Wh/L)**	**Nominal Voltage (V)**	**Number of Charging Cycles**
Nickel–cadmium (Ni-Cd)	40–60	50–150	1.25	1500
Nickel–metal hydride (Ni–MH)	60–120	140–300	1.25	500–1000
Lithium–ion (Li–ion)	100–265	250–730	3.6	400–1200

[a] *Battery rating from Soykan (2002)*
[b] *http://www.panasonic.com/industrial/batteries-oem/oem/lithium-ion.aspx*
[c] *http://batteryuniversity.com*

silver-oxide (button cell types or watch batteries). Implantable medical devices now rely on the reliable lithium chemistries for long service life (proven for decades on pacemakers).

From Tables 2.2 and 2.3, it is evident that primary cells have higher capacity (specific energy and energy density) than secondary cells. It is not surprising that primary cells are typically employed for implanted devices, while secondary cells are commonly used for inductive links (externally). While the first pacemaker batteries were made from mercury cells; nowadays the service life of lithium-based primary cells makes them obvious candidates for long-term biomedical implants. Sadly, primary cells do not fare well when compared against gasoline. (Specific energy of 13,000 Wh/kg or energy density of 9,700 Wh/L. Gasoline is at least one order of magnitude higher than the highest primary cell.) However, for some combustion engines, primary cells are about the same level (Figure 1.2). Secondary cells are limited by the number of charging cycles they undergo before significantly losing capacity. Most importantly, they release heat when recharging which is not acceptable for medical implants. Thus, primary cells are without doubt the best powering alternative for implantable medical devices.

2.2 ENERGY GENERATION FROM THE HUMAN BODY

The human body is a machine that burns 2,000–2,500 food calories per day in order to function appropriately. One food calorie or Calorie (with upper case) is equal to 1,000 calories (with lower case), where 1 calorie is equivalent to 4.19 J of energy. Thus, 2,000–2,500 Calories correspond to 8.4–10.5 MJ in energy, or 2.3–2.9 kWh power consumption, a relatively large number of energy (the same energy consumption

of two small microwave ovens at full capacity for 1 h). About 20% of this energy is converted into mechanical work and most leaves the body as wasted heat (in order to keep the body warm). Therefore, it is not surprising that research has focused into harnessing energy from either body activities or heat waste (temperature difference).

Active power generation produces significantly higher power output, as evidenced by bicycle generators powering small TV sets. For example, an occasional cyclist can produce close to 150 W, but a professional can output on average up to 700 W (Flipsen, 2006). Some studies in this area have covered the power outputs expected from some activities, such as cranking, shaking, and pedaling, as well as the comfort of sustained generation. Jansen and Stevels (1999) reported active power generation levels using lever-driven generators (~6 W), crank-driven generators (~21 W), and bicycle pedaling (~100 W). Later work from this group (Slob, 2000) studied the power generation from sustained one-hand cranking. It was presented that power output drops close to 40 W from a peak of 150 W after 10 min of continuous cranking. It was concluded that 28 W on average can be obtained from sustained cranking for 30 min and that 14 W could be converted into electricity if assuming a conversion mechanism efficiency of 50%. Other examples studied include the peak power from cycling and rowing as 600 and 800 W, respectively, but they are reduced to near 20% after 5 min of continuous activity[1].

One of the first reviews on energy generation from the human body was made by Starner (1996). The description included analysis for available power from body heat (0.2−0.3 W on the neck, 0.6−1.0 W on the head, and 3−5 W on the entire body surface), respiration (~1 W for breathing, ~0.8 W from chest movement), blood pressure (~1 W), and other activities, such as typing (0.007−0.02 W), bicep curls exercising (~20 W), arm lifting (~60 W), and walking (~70 W). Although those numbers and locations represent an expected average power limit, devices harnessing those power levels could interfere severely with everyday activities but devices harvesting a small percentage of those levels can be a feasible option.

Acceleration and step frequency were evaluated to determine how much energy can be available at different body locations and at

[1]http://web.kyoto-inet.or.jp/people/kazuho/manasle/manasle.htm. Retrieved January 29 2013.

different walking and running speeds (Romero et al., 2011). Energy harvesters can then be designed to scavenge this energy for powering portable electronics or implantable biomedical devices.

2.3 POWER LIMITS

Energy harvesting generators harnessing motion typically follow a cantilever-beam architecture with a proof mass at the end of the beam, although several other geometries are also used, as shown in Figure 2.1. This approach that uses a proof mass are known as inertial or kinetic energy harvesting. The transduction from kinetic energy to electrical energy usually consists of electromagnetic, piezoelectric, or electrostatic technique. Electromagnetic generation uses the relative displacement between a magnet and a coil to induce a voltage; piezoelectric generation uses the straining of the material to produce a voltage; whereas electrostatic transduction uses the changing distance of the parallel plates of a capacitor (or change of dielectric properties) to increase the voltage (potential energy) of a charged capacitor. Mitcheson et al. (2004b) classified the kinetic generators according to the damping mechanism used. Hence, generators are classified according to the damping by a force proportional to the velocity, velocity-damped resonant-generators (VDRGs), or by a constant force, Coulomb-damped resonant-generators (CDRGs). Coulomb-force parametric-generators (CFPGs) is the category for nonresonant generators damped by a constant force. Electromagnetic and piezoelectric transductions are the common methods for VDRGs, while CDRGs and CFPGs usually employ electrostatic transduction.

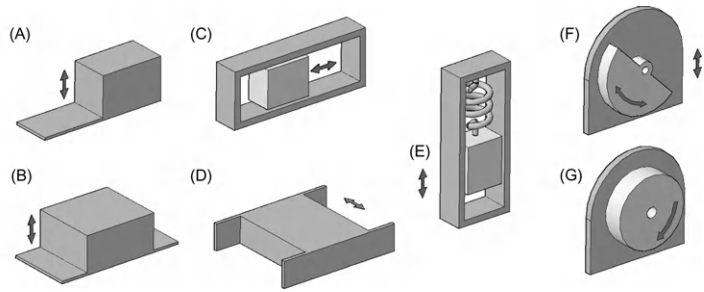

Figure 2.1 Energy harvester geometries: (A) cantilever beam, (B) out-of-plane plate, (C) free-sliding mass, (D) in-plane plate, (E) spring–mass system, (F) oscillating rotational, and (G) continuous rotation generator. Designs adapted from Yeatman et al. (2007) and Arnold (2007).

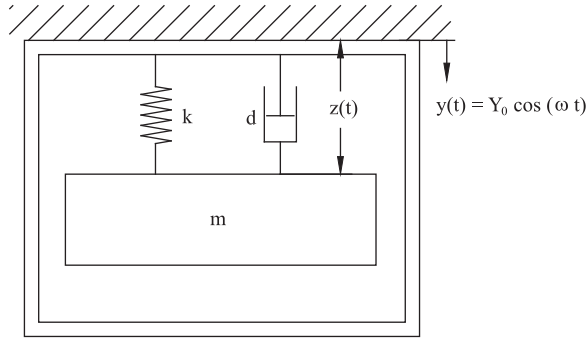

Figure 2.2 Schematic of kinetic energy harvester.

A typical schematic of a kinetic energy generator is shown in Figure 2.2. This arrangement, a spring−mass system, consists of a proof mass m, a spring with constant k (sometimes shaped as a cantilever beam), and a damper d (that encompasses frictional and energy generation damping terms). The spring−mass system is represented as

$$m\ddot{z}(t) + d\dot{z}(t) + kz(t) = -m\omega^2 Y_0 \sin(\omega t) \tag{2.1}$$

where z is the relative displacement, ω is the frequency in rad/s, and Y_0 is the vibration amplitude. The steady-state solution, as presented by Rao (1995), for a sinusoidal-driven input function is

$$z(t) = \frac{Y_0 \omega_r}{\sqrt{(1-\omega_r^2)^2 + (2\zeta_t \omega_r)^2}} \sin\left(\omega t - \left(\tan^{-1}\left(\frac{d_t \omega}{k - m\omega^2}\right)\right)\right) \tag{2.2}$$

where ω_r represents the ratio of input frequency to natural resonant frequency $\omega_r = \omega/\omega_n$, ω_n is the natural resonant frequency ($\omega n = \sqrt{}$ km), ζ_t is the total damping ratio ($\zeta_t = d_t/(2m\omega_n)$), d_t represents the total damping, while tangent term inside the last parenthesis is the phase angle.

The power dissipated from the system represented in Figure 2.2 into the damper, from El-Hami et al. (2001), is

$$P_d = \frac{m\zeta_t Y_0^2 \omega_r^2 \omega^2}{[1-\omega_r^2]^2 + [2\zeta_t \omega_r]^2} \tag{2.3}$$

The maximum power is found when the vibration frequency matches the natural resonant frequency ($\omega_r = 1$). The previous expression becomes

$$P_d = \frac{1}{2} m Y_0^2 \omega_n^3 \frac{1}{2\zeta_t} \tag{2.4}$$

Using the expression $a = Y_0\omega^2$, where a is the acceleration of the system, the previous equation can be rewritten as

$$P_d = \frac{1}{2} m \frac{a^2}{\omega} \frac{1}{2\zeta_t} \tag{2.5}$$

where the last term is also known as the Q factor ($Q = z/Y_0 = 1/(2\zeta)$) leading to

$$P_d = \frac{1}{2} m \frac{a^2}{\omega} Q \tag{2.6}$$

Yeatman (2008) described four limiting parameters for energy generation: the proof mass m, the input displacement amplitude Y_0, the proof mass displacement z, and the vibration frequency ω. For example, from Eq. (2.5), high-frequency vibrations would produce a higher power output, but high-frequency acceleration is commonly related to small displacements and relatively low accelerations. In considering the inherent relationship between acceleration a, frequency ω, and displacement Y as $a = \omega^2 Y$, the limiting parameters are further restricted. Because the acceleration, frequency, and displacement are given by the external vibrating source, rather than being of free selection, the energy generation parameters are reduced to three. Then, the relevant factors are the acceleration-squared-to-frequency (which is an input source constraint), the proof mass m (a sizing factor), and the Q factor (a generator design constraint).

The acceleration-squared-to-frequency term will be referenced as $ASTF$ or σ_ω, which will also be considered as a figure of merit for the energetic content of the source (m^2/s^3 units) and equal to

$$\sigma_\omega = \frac{a^2}{\omega} \tag{2.7}$$

The Q factor is a dimensionless parameter that relates the total energy stored to the energy lost in a single cycle. The Q factor is then a measure of the quality of an energy harvester. Conversely, the $ASTF$ or the σ_ω term represents the energy level from the source. Therefore, energy harvesters are ultimately limited by the level of energy from the source (σ_ω) and by the energy generation process (Q factor). Thus, Eq. (2.6) can be written as

$$P_{\text{available}} = \frac{1}{2} m \sigma_\omega Q \tag{2.8}$$

Table 2.4 ASTF Values Calculated from Various Motion Sources

Vibrating Source	σ_ω (m^2/s^3)
Base of a three-axis machine tool[a]	0.230
Blender casing[a]	0.054
Cloth dryer machine[a]	0.016
Washing machine[a]	0.0004
Small microwave oven[a]	0.007
Home breadmaker[a]	0.001
Heating, ventilation, and air conditioning (HVAC) vents in office building[a]	0.0001–0.006
Walking (measured on the head) [b]	0.5–3.0

[a] *Calculated from Roundy (2003).*
[b] *Calculated from Hirasaki et al. (1999).*

Roundy (2003) provided some examples of the peak acceleration and its corresponding frequency for several applications; these results are tabulated for σ_ω values and summarized in Table 2.4. A study by Hirasaki et al. (1999) provided values from acceleration and frequency from human walking to tabulate the σ_ω term presented in Table 2.4. From these results, the $ASTF$ (or σ_ω values) for machine-based vibrations are relatively low ($\ll 1$). In contrast, σ_ω values from body activities, such as walking, are relatively high (>1).

Stephen (2006) reported that electromagnetic energy harvesting can deliver a maximum power that corresponds to 50% of the maximum available power. Therefore, the expression for maximum power that can be delivered into the electrical load is

$$P_{\text{max elect}} = \frac{1}{4} m \sigma_\omega Q \tag{2.9}$$

Arranging previous equation to be divided by the generator volume V to obtain volumetric power density, such as $V = m/\rho$, where ρ is the proof mass density, leads to

$$\frac{P_{\text{max elect}}}{V} = \frac{1}{4} \rho \sigma_\omega Q \tag{2.10}$$

A plot of the last equation is shown in Figure 2.3. A proof mass density of 10 g/cm^3 was used (for simplicity and because it is similar to that of molybdenum). Two distinct zones are displayed, the first is for the human-based motion harvesters (assuming $Q \sim 1$ and $\sigma_\omega \sim 1$), while the second is for machine-based vibration generators (assuming

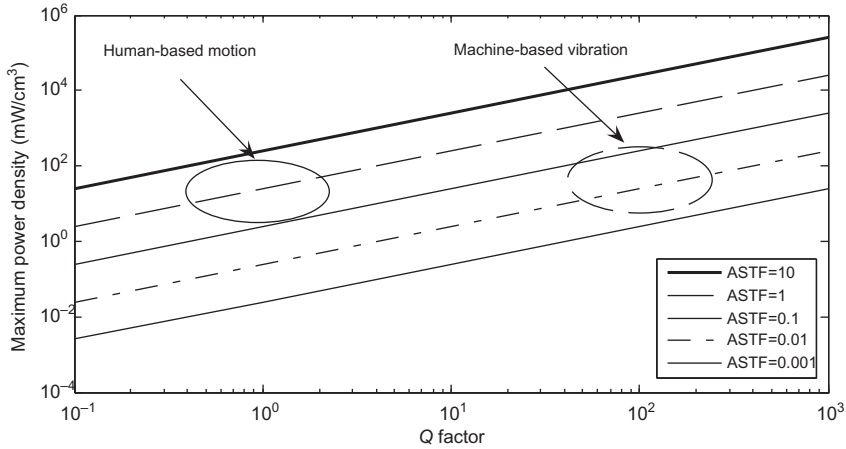

Figure 2.3 Maximum power available for linear-vibration generators at resonance from human-based motion and machine-based vibration.

$Q \sim 100$ and $\sigma_\omega \sim 0.01$). The σ_ω values from Table 2.2 served as reference.

Figure 2.3 indicates the maximum power that can be delivered into an electric load for a system vibrating at its resonant frequency. If the energy from body motion can be harnessed by operating at resonance, then power densities comparable to generators from machine vibrations can be reached. From Figure 2.3, it seems reasonable to generate power from body motion with power densities on the order of milliwatt per cubic centimeter. Therefore, human-based generators are still an untapped source of kinetic energy.

However, Figure 2.3 only gives an estimate of where the overall maximum power density lies. The values must vary depending on body location and type of activity performed. A study performed by Romero et al. (2010) evaluated several body locations (ankle, knee, hip, chest, wrist, elbow, upper arm, and side of the head) while walking and running on a treadmill. This evaluation provided an approximation of the maximum available power. The test was performed on 10 individuals (5 women, 5 men) with accelerometers strapped at those locations and a portable data logger. Treadmill walking speed varied from 1.0 to 4.0 mph (0.45−1.79 m/s) while running speeds ranged from 2.0 to 5.0 mph (0.89−2.24 m/s). Three-axis accelerometers ($\pm 3G$[2]

[2] $1G = 9.8$ m/s^2.

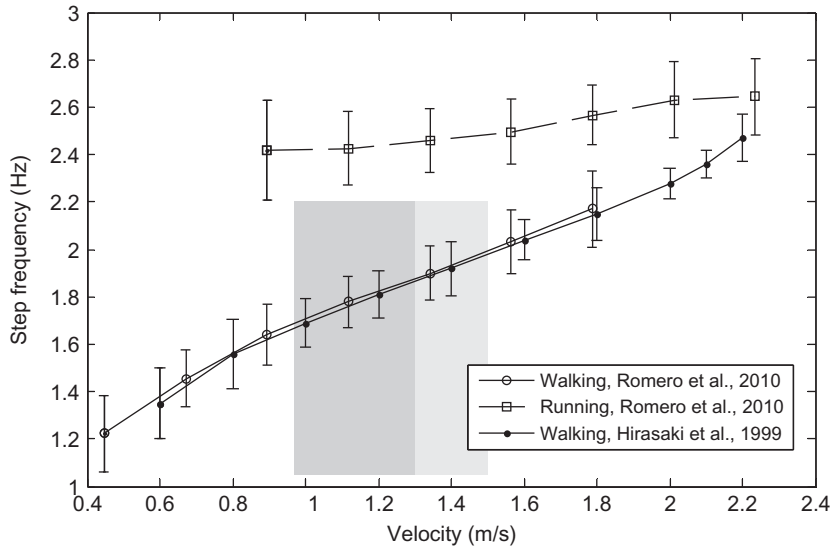

Figure 2.4 Step frequency for the walking and running test on a treadmill. Error bars represent one standard deviation. Darker shaded area represents the 15th-percentile up to the average walking speeds for older pedestrians (over 65 years old), while the clear-shaded area includes for the 15th-percentile up to the average walking speeds for younger pedestrians (14–64 years old). Average walking speeds of older and younger pedestrians from Knoblauch et al. (1996).

ADXL335 and $\pm 6G$ MMA7260Q) and two-axis accelerometers ($\pm 18G$ ADXL321) were employed and 60 s recordings were performed at each speed.

The stride frequency results are presented in Figure 2.4 for the walking and running tests (error bars represent one standard deviation). Step frequencies for the walking test varied relatively linearly from 1.2 to 2.2 Hz (1–4 mph). A 1% variation in the step frequency was found when this test was compared against that of Hirasaki et al. (1999), as shown in Figure 2.4. The average walking velocity of 1.4 m/s ($\sim$3.1 mph) was found to have an associated step frequency of 1.9 ± 0.1 Hz, while the running test showed an almost constant step frequency of 2.5 Hz. The shaded regions were added for comparison purposes for older and younger pedestrian average walking speeds. Average walking speed has been reported to be 3.4 mph ($\sim$1.5 m/s) for younger pedestrians and 2.8 mph ($\sim$1.3 m/s) for older pedestrians (over 65 years old), while the 15th-percentile was 1.25 m/s for younger pedestrians and 0.97 m/s for older pedestrians (Knoblauch et al., 1996).

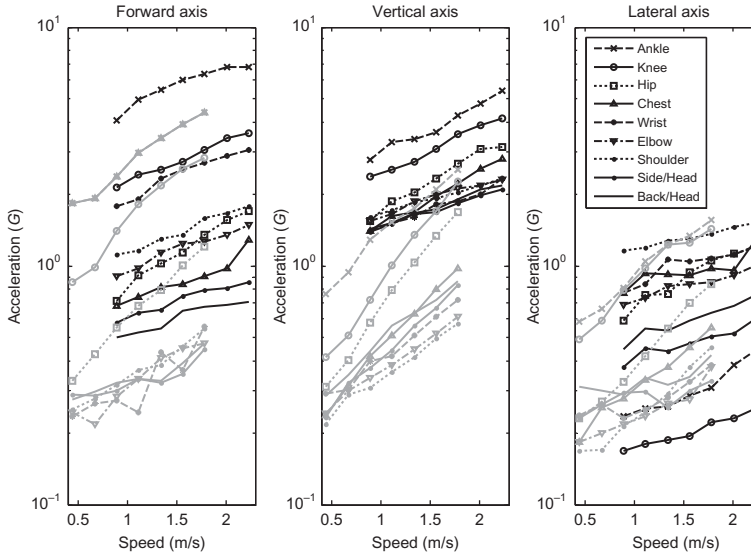

Figure 2.5 Acceleration readings comparison from the walking (gray color lines) and running (black color lines) test at each body location in G *(1*G *= 9.8 m/s^2). Walking test: 10 subjects, age: 29.4 ± 5.8, height: 1.68 ± 0.1 m, weight: 62.9 ± 12.8 kg. Running test: 10 subjects, age: 28.7 ± 7.08, height: 1.68 ± 0.1 m, weight: 63.2 ± 12.4 kg.*

The acceleration results for the different body locations are presented in Figure 2.5 for the walking and running test for each individual axis. It is shown that high energetic locations (those that undergo abrupt movements, such as the ankle and knee) exhibit larger accelerations than other body locations. The larger accelerations were seen on the knee ($\sim$1 to $\sim$3G) and ankle ($\sim$2 to $\sim$4.5G) locations for the forward direction while walking. Acceleration variation for the same locations ranged from $\sim$1 to $\sim$2.5G for the ankle and from $\sim$0.5 to $\sim$2.5G for the knee (walking test). Most other body locations had accelerations while walking ranging from $\sim$0.3G up to about 0.5−1G. These values are similar in magnitude at most locations of the vertical and lateral axes (except ankle, knee, and the hip to some extent). Lower body locations (ankle, knee, and hip) had a larger acceleration component along the vertical axis. Acceleration for the average walking velocity of 1.4 m/s ($\sim$3.1 mph) was close to 0.5G for most of the body locations (except the ankle and knee). Acceleration readings were larger for running than for walking. Forward and vertical axes presented larger accelerations than the lateral axis. While running, lateral axis accelerations (0.2−1.2G) exhibited little variation at all speeds. The forward direction had acceleration readings from $\sim$4 to 7G for

Table 2.5 Energetic Figure of Merit, σ_ω, for the Average Walking Speed of 1.4 m/s (3.1 mph) and for the Moderate Running Speed of 2.2 m/s (5 mph)

Body Location	Walking			Running		
	Forward Axis (m^2/s^3)	Vertical Axis (m^2/s^3)	Lateral Axis (m^2/s^3)	Forward Axis (m^2/s^3)	Vertical Axis (m^2/s^3)	Lateral Axis (m^2/s^3)
Ankle	10	2.7	1.3	27	17	0.2
Knee	4	1.6	1.3	7	10	0.1
Hip	0.6	1.0	0.3	1.7	6	0.8
Chest	0.4	0.4	0.1	1	5	1
Wrist	0.15	0.23	0.07	6	3	0.8
Elbow	0.15	0.18	0.05	1.3	3	0.6
Shoulder	0.15	0.15	0.05	2	3	1.3
Side of the head	0.1	0.28	0.05	0.5	2.5	0.3
Back of the head	0.1	0.32	0.08	0.4	2.7	0.3

the ankle and from $\sim$2 to 3.5G for the knee and wrist. The other body locations ranged from $\sim$0.7 to $\sim$1.5G along the forward axis, while varying from $\sim$1.5 to $\sim$2.5G for the vertical axis. The higher accelerations were found along the vertical axis rather than the forward axis, except for the ankle. More detailed information can be found in Romero (2010).

The energetic figure of merit for the different body locations is summarized in Table 2.5. Available power can be estimated from Eq. (2.7) using the findings from the energetic figure of merit σ_ω. A first estimation is made assuming a generator with a 1 g proof mass and a Q factor of 1, as shown in Figure 2.6. From the walking test, available power levels below 0.5 mW are expected for most of the body locations, while the ankle and knee positions are able to provide higher power levels. During the running test, the available power increases to over 0.5 mW for most of the body locations along the vertical axis, while the ankle and knee present significantly higher values.

A second estimation is based on the power density metrics of Eq. (2.10) assuming a proof mass density of 10 g/cm^3 and a Q factor of 1. Figure 2.7 shows the power densities for each body location at different walking and running speeds. From these results, most of the body locations provide less than 1 mW/cm^3 from walking, while

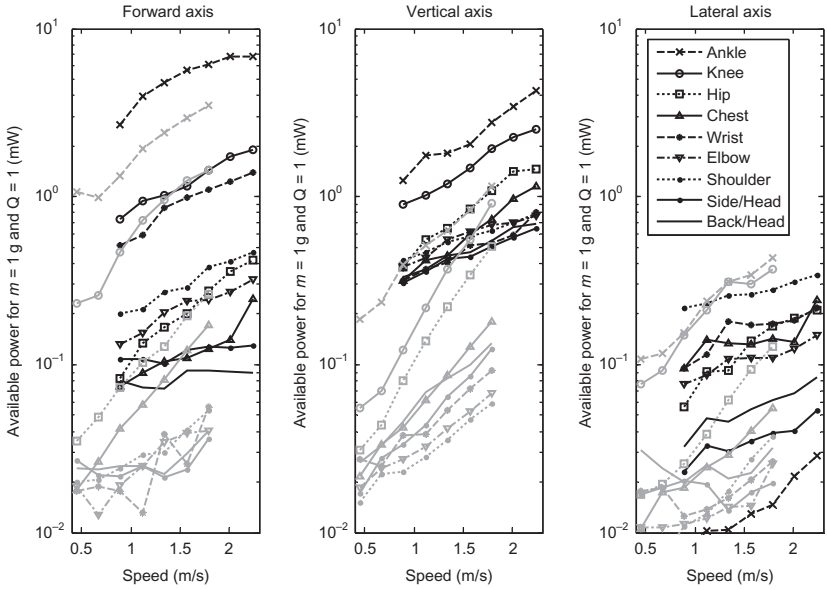

Figure 2.6 Available power comparison at different body locations from walking (gray color lines) and running (black color lines) for an energy harvester with 1 g proof mass and a Q factor of 1.

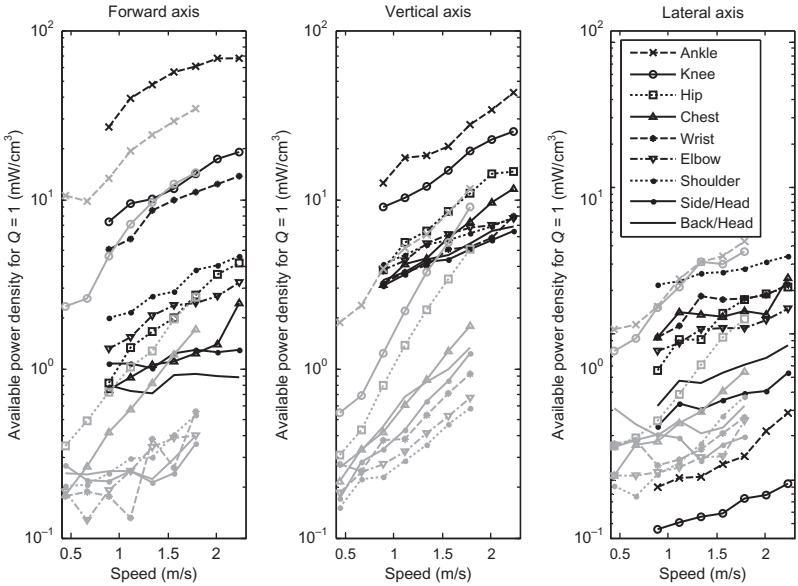

Figure 2.7 Available power density comparison at different body locations from walking (gray color lines) and running (black color lines) for an energy harvester with $\rho = 10$ g/cm^3 and a Q factor of 1.

supplying over 1 mW/cm^3 from running. The ankle location has an associated power density as high as 25 mW/cm^3 from walking and as high as 68 mW/cm^3 from running.

A linear energy harvester could use the forward, vertical, or lateral motion of a walking or running individual to generate power according to the analysis provided. Larger amounts of power output can be achieved if energy is harvested from several axes at the same time. A generator design employing the three acceleration components for energy generation would be relatively difficult to accomplish while remaining small in size (with relatively large dimensions along the three axes). An energy harvester using two of the acceleration axes would benefit from a planar design which is more appropriate for surgical implantation or for portable electronics. A planar topology can be accomplished by using two individual linear generators, one linear generator aligned to the resultant acceleration vector or a rotational approach. As the lateral axis has smaller acceleration components, a resultant vector formed by the forward and vertical axes will have a larger magnitude.

As a comparison, power can also be estimated using the mechanical work W and the frequency f as

$$P = Wf \tag{2.11}$$

where the work W of a mass m along a distance d against the Earth's gravity g is $W = mgd$. Considering the average vertical displacement while walking to be 5 cm (Rome et al., 2005), the work done by a 1 g mass is $\sim$0.5 mJ. Then, the power associated at a walking frequency of 2 Hz is $\sim$1 mW but only half of that can be converted into electricity (Stephen, 2006). This result is at the same power level as the one presented. In summary, a 1 g proof mass generator traveling 5 cm at 2 Hz has an available power content of $\sim$0.5 mW. Thus, a larger device could produce more than 0.5 mW, and a smaller energy harvester would produce only a fraction of that. As it could be expected, larger energy harvesters can produce a larger power output, thus generators can be sized according to the power required for implantable or portable electronics.

In summary, available power density is found to be over 0.5 mW/cm^3 for most of the body locations while walking (ankle and knee present higher magnitudes). Running gives power density levels

over 3 mW/cm^3 for all body locations (the ankle location could be over 100 mW/cm^3). Some biomedical devices have power requirements similar to what is theoretically available (cardiac pacemakers require an average of 0.1 mW, while hearing aids consume around 0.05 mW, Flipsen et al., 2004). Therefore, some biomedical applications can benefit directly from this energy harvesting approach for their power. Yet, most devices are still far from these theoretical values.

CHAPTER 3

Enabling Technologies

In addition to energy generators that have been presented previously in the literature (Beeby et al., 2006; Cook-Chennault et al., 2008; Paulo and Gaspar, 2010; Romero et al., 2009), there are novel approaches that encompasses chemical (e.g. direct glucose fuel cells), thermal, and nano-generators. An updated review of the latest research development for biomedical applications is discussed. Thermal generators require a thermal gradient to operate. This makes them impractical for deep implants where thermal gradients can be as high as 0.2°C but when placed at the skin surface they can have temperature differences from 1°C to 5°C. For example, 1°C of temperature gradient can be enough to produce up to 100 μW of power on average, which should be enough for powering a cardiac pacemaker. New advances in nanotechnology promises even smaller devices for implantable applications. Nanowires made of zinc oxide (a nontoxic piezoelectric material) can be manufactured into a flexible implantable material that can harness the veins pulsations inside the body to power heart beat and blood pressure monitors (Yang et al., 2009). Biological fuel cells, or direct glucose fuel cells, using glucose rather than nitrogen can be a possibility. Nishizawa et al. (2005) presented this approach fabricating a coin-sized biofuel cell that generated up to 140 μW of power.

3.1 CHEMICAL ENERGY

Direct glucose fuel cells, also known as biofuel cells, can use glucose as a fuel. The main advantage is that when using blood glucose for energy generation, it produces water as byproduct. A biofuel cell prototype capable of producing up to 140 μW of power was presented by Nishizawa et al. (2005). However, these types of biofuel cells (enzymatic type) are challenged by the short lifetimes, in the order of several weeks, and by inefficient fuel oxidation (Barton et al., 2004; Minteer et al., 2007). Biological batteries, using biological fluids, have also been reported. Lee (2005) developed a low-cost paper laminated battery (dimensions of 60 mm × 30 mm) using copper and magnesium as the electrodes and a chloride-doped filter paper. This battery is activated

when droplets of urine (or other acid fluid, even apple juice) interacts with the doped paper. This battery produced power as high as 1.5 mW, with a voltage of 1.5 V. As the battery can be manufactured and integrated with bioMEMS, the author suggests that applications involving urine samples can routinely monitor patient's physiological responses. Potential additional applications related to home-base health kits and biosensors. Interestingly enough, this battery is actually found in the market in Japan in AA and AAA size presentations[1].

3.2 THERMAL ENERGY

Thermal energy generation is limited by the Carnot efficiency equation (see Eq. 1.4 in Chapter 1). Taking the body temperature as the T_{high} term at 37°C (310 K), and using outdoor temperatures of 27°C (300 K) and 20°C (293 K) for the T_{low} term into Eq. (1.4) allows for efficiencies ranging from 3.2% to 5.5%. Although theoretical numbers, they are quite low for efficient energy generation. Today, thermoelectric materials offer efficiencies on the order of 1% for temperature gradients under 20°C (Starner and Paradiso, 2004).

The human body radiates around 300 W of power as heat. If all body heat could be used for energy generation with efficiencies between 3% and 5%, 9–17 W of power could be harvested. The extraction of all body heat would require wearing a special suit that could not be comfortable to carry. Thus, using a smaller area for power generation, about 5% of body (similar to the neck area), a maximum of 0.4–0.8 W could be produced. Increasing the exposed area to include the head from 0.6 to 1.0 W of electrical power could be recovered. Commercial devices have been using this technology in a number of products. The Citizen TEG wristwatch is capable of producing up to 13 $\mu W/cm^2$ using a temperature difference of 1°C (Flipsen, 2005), while the Applied Digital Solution's Thermo Life Generator can produce up to 60 $\mu W/cm^2$ with a temperature gradient of 5°C (Paradiso and Starner, 2005). Researchers have also being able to show that a subcutaneous temperature gradient of 0.3–1.7°C can generate more than 70 μW of power (Watkins et al., 2005). This is about the same level as the power requirements for some pacemakers. Mateu et al. (2007) presented an investigation where an externally mounted thermoelectric

[1] http://www.theregister.co.uk/2007/09/04/nopopo/.

generator delivered 2 mW of power for a temperature difference of 7°C (dimensions of 2.5 cm × 2.5 cm with an added heat sink).

3.3 KINETIC ENERGY

Harnessing daily activities such as walking for passive energy generation is a well-documented topic. For instance, backpacks, the footfall, the swinging of the legs have been studied and devices have been designed. Items vary from large devices to those that can be carried in a pocket.

Backpacks have been engineered for energy generation. Rome et al. (2005) employed the up-and-down movement of backpack loads to generate energy. This backpack design was divided in two frames: a vertical-moving structure where the load was placed and a fixed frame attached to the individual. A toothed rack on the moving frame was connected to a gear box on the fixed structure, which was attached to a DC generator. When the movable structure traveled 4.5 cm, the generator could rotate up to 5,000 rpm due to the gear box. Power generation up to 7.4 W was reported when carrying heavy loads (38 kg). In addition, the load peak force from the movable design decreased up to 12% when compared to a fixed cargo. This decrease in the metabolic cost increases the efficiency of the overall energy generation process.

A study of backpack straps as locations for piezoelectric generators was undertaken by Feenstra et al. (2008). The tension force on the straps, with the stacks placed in series, was mechanically amplified and converted into compressive load. It was reported a power generation of 176 μW when walking on a treadmill with a 40 lb load, while the maximum power output is expected to be on the order of 400 μW. Although this number seems small, it also requires minimal backpack modification, enough for sensing capabilities.

Li et al. (2008) presented a knee-mounted brace for biomechanical energy harvesting during walking. A gear train and a small permanent magnet generator were fitted on a custom knee brace. This generator was designed to harness the energy from leg deceleration rather than for continuous generation, similar to the generative braking process of hybrid cars. The gait process is divided into two stages: swing and stance. At the swing phase when the leg is moved forward, the body uses energy to decelerate the limb. This generator, when operated under the right conditions, was able to produce a power peak close to

20 W and an average power output of 4.8 ± 0.8 W. This generative breaking was reported to use less than 1 W of metabolic power to produce 1 W of electrical power, while if used continuously more than 2 W of body work are needed to generate only 1 W of usable power.

A piezoelectric generator for powering artificial organs harnessing the footfall during gait was presented by Antaki et al. (1995). This generator consisted of two hydraulic cylinders placed in a shoe insole containing lead zirconate titanate (PZT) piezoelectric stacks. The hydraulic cylinders had pulse amplifiers beneath the toes and heel region for transforming the low-frequency footfall into high-frequency pulses. A 1/17 scale prototype was evaluated producing 150−675 mW for walking (5.7 ± 2.2 mWkg/L) and 675−2,100 mW (23.6 ± 11.6 mWkg/L) for simulated jogging, while up to 6.2 W could be expected from a 75 kg individual.

The bending of the shoe has been studied as well. A flexible piezoelectric generator was developed by Kymissis et al. (1998). They have introduced the concept of parasitic power generation capturing the energy that otherwise would be wasted or dissipated. For example, a 68 kg individual walking at 1 Hz with a 5 cm vertical displacement represents 67 W of power employed (Starner and Paradiso, 2004). Trying to harvest all the energy would severely interfere with the gait process but using the deformation that a sports shoe suffers (less than 1 cm) seemed practical. Kymissis et al. (1998) presented two different piezoelectric designs to be compared against an electromagnetic generator. The first configuration was made of a stack of polyvinylidine-fluoride (PVDF) sheets shaped similar to a shoe sole to be stressed under bending (the outside layers were stretched while the inner layers were compressed). This arrangement provided ± 60 V with an average power output of 1.1 mW. The second configuration was designed to harness the heel strike using a unimorph strip (steel spring bonded to a PZT piezoelectric material sheet). The steel was bent stressing the PZT when there was a heel strike, generating peak voltages up to 150 V and power outputs up to 1.8 mW. The electromagnetic design was made from a lever-driven flashlight generator mounted in a shoe. A hinged plate attached to the flashlight lever exploited 3 cm of walking stroke producing an average power output of 230 mW, although interfering with the normal gait. The piezoelectric shoe generators were also used as Radio-frequency identification (RFID) transmitters sending a 12-bit

serial ID at 310 MHz every 3–6 steps up to a 20 m distance. Later work described a power output of 1.3 mW for the PVDF stack and 8.4 mW for two back-to-back unimorphs (Shenck and Paradiso, 2001). Similar work from this group used push buttons with piezoelectric materials. These push buttons (commercial piezoelectric strikers connected to amorphous-core transformers) produced 0.5 mJ of energy at 3 V for transmitting 12-bit ID code over 30 m several times (Paradiso and Feldmeier, 2001).

Heartbeats have been ideated as well for devising generators using piezoelectric materials. A patent granted in 1969 to Wen H. Ko described one of the first attempts to harness heart motion for electric generation. This generator described by Professor Ko was a piezoelectric rectangular-shaped cantilever beam with an added weight at its free end. The structure when vibrating at a suitable frequency produced a signal rectified by a voltage doubler. This design was intended to power an electrical implant such as a cardiac pacemaker. This piezoelectric device was tested on a dog's heart beating at 80 bpm producing a 4 V output voltage on a 105 Ω load for 160 μW of power. Edward A. Schroeppel's patent (1987) described a different approach when trying to harness the heart motion to power a cardiac pacemaker circuit. This patent described a piezoelectric strip inside a catheter for human heart insertion. When the heart is beating, it bends the catheter which stresses the piezoelectric strip generating an output signal.

The first commercial oscillating rotational generators originated from wristwatch companies. The Japanese company Seiko presented the Automatic Generating System (AGS) in 1986. This self-winding mechanism was used on wristwatches under the Kinetic brand name. The design consisted of a rotating pendulum mass, a gear box train (ratio 1:100), and a small permanent magnet generator. Due to wrist position changes, one oscillation from the pendulum mass produced 100 rotations on the generator. According to Paradiso and Starner (2005), 5–10 μW of power was estimated to be produced when worn and 1 mW could be obtained when forcibly shaken. Swiss company ETA later introduced the Autoquartz with a different approach. The pendulum mass wound a spring connected to a small generator using a gear box train. Once the spring was fully wound, it unwound making the generator rotate at 5–15 krpm for a short time (50 ms), generating more than 15 V and 6 mA (90 mW) (Paradiso and Starner, 2005).

Researchers have also investigated commercial wristwatch generators to determine if it is possible to use them for implantable biomedical applications. For example, Goto et al. (1998, 1999) exploited the Seiko's generator for powering a circuit to pace the heart of a dog. The generator, when placed for a 30 min period on the right ventricular wall of a dog's heart beating at 200 bpm, was able to store 80 mJ of energy in a capacitor. Another test using a charged capacitor was capable of pacing a dog's heart at 140 bpm for 60 min consuming 420 mJ. The actual energy requirement of 210 mJ for 30 min was higher than the energy produced in the same amount of time, 80 mJ. The 13 μJ of energy produced was compared against a cardiac pacemaker requiring only 5 μJ (2.5 V, 0.4 ms, and 500 Ω load). This showed the feasibility of generating the power needed for the stimulation. No long-term studies were presented considering the possible effects of the generator on the heart wall. Later work from Gorge et al. (2001) tried to determine how much power could be generated using the Seiko's generator taped to the chest of individuals working in an office environment. It was concluded that, over a period of 8 h, the power generated varied from 0.2 to 2.1 μW, with a mean value of 0.5 μW. This power level was considered to be 10−100 times less than required for charging a cardiac pacemaker battery.

Further studies employing the Seiko generator have also been undertaken. The analysis performed by Sasaki et al. (2005) found that if the right conditions are given to keep the rotations, this generator can produce up to 10 times more energy than from swinging motion alone. A swinging motion at 1 Hz was found to produce 15 μW, while self-excited rotations were able to produce up to 170 μW at 2 Hz. The conditions to maintain these rotations were described as

$$|\dot{\theta}|_{t=0} > \omega \tag{3.1}$$

$$\frac{2c}{Ama\omega} < 1 \tag{3.2}$$

where θ is the rotation angle, ω is the angular speed, c is the electromagnetic damping, A is the amplitude of the external oscillation, m is the pendulum mass, and a is the distance between the center of gravity and the axis of rotation. Another promising linear generator was also presented by this group. It was composed of a permanent magnet mass suspended by springs and surrounded by a 400-turn coil. Although the linear generator had an overall volume of 500 cm^3, it was reported

that it produced up to 90 mW when excited at its natural resonant frequency of 6 Hz with a vibration amplitude of 5.5 mm.

Wang et al. (2005a) have also improved upon the original Seiko design. Their objective was to increase the power output density from about 7.5 to 50 mW/cm^3. This group fabricated a miniature eight-pole permanent magnet generator using an imbricated-pole stator with a single wire-wound coil to be driven at high speed. A prototype generated 15 mW at 6,000 rpm (100 Hz) after rectification by a Schottky-diode bridge for a volume slightly larger than 1 cm^3.

In addition to the rotational design from wristwatches, linear displacement generators, similar to the commercial shake-driven flashlights, have also been investigated for body motion. Duffy and Carroll (2004) described one such design situated inside a shoe sole. The generator was composed of two opposing magnets attached together inside a container with three wrapped coils, about 45 mm long and 13 mm in diameter. The shoe generator produced 8.5 mW when tested at a frequency of 5 Hz. A second generator design consisting of a set of fixed magnets facing a moving magnet with a coil in between was also tested. This set was able to produce up to 230 μW of power at a frequency of 5 Hz. Further work (Duffy and Carroll, 2005) evaluated different rectification circuits: half- and full-wave designs versus doubler and quadrupler voltage multipliers. The doubler was found to produce a higher voltage and power output. A six-coil design with sliding magnets produced peak-to-peak voltages of 4 V (400 mVrms) when tested at 2 Hz. The voltage doubler offered a rectified power output close to 1 mW when using a 0.1 F double-layer capacitor; although up to 2 mW was expected. It was assumed that this was due to the capacitor taking longer to charge.

Studies made by Niu and Chapman (2006) evaluated arm swinging, foot movement, and trunk displacement as potential locations for energy harvesting. Their proposed design used a linear electromagnetic generator tested on the mentioned body locations. An average power output of 10 mW and an open-circuit peak voltage of 7 V were reported for the device placed on the arm. A backpack-situated generator produced 50–80 mW with a peak voltage of 20 V (open circuit), while the power output for the harvester worn on a shoe was 80 mW for an open-circuit peak voltage close to 27 V. Power was measured after rectification while charging a battery. It was reported that impedance matching would increase the power by a factor of 3.

Linear electromagnetic generators have also been optimized for energy harvesting while walking, as performed by von Buren and Troster (2007). The generator consisted of an air-core tubular structure having a flexure bearing and a free-sliding magnet stack surrounded by coils. Energy harvesters having a volume of 0.25 cm^3 were analyzed with different quantities of magnets (6–9) and coils (6–10). The power output varied according to the body location but on average 2–25 μW was recorded. A comparison was offered with a lithium–ion battery having an energy density of 0.3 Wh/cm^3. The battery would be depleted in a 4-year period if 2 μW is drawn, or its energy would be completely consumed in 4 months if the power drain is 25 μW. A prototype with a volume of 0.5 cm^3 (15 mm long, 6 mm diameter) having 6 magnets and 5 coils was tested below the knee while walking for an average output power of 35 μW and a peak power of 1 mW (electrical efficiency of 66% on a 10 Ω load).

Another study employing a linear electromagnetic generator (55 mm long, 17 mm diameter) using a free-sliding magnet surrounded by coils was presented by Saha et al. (2008). Two different configurations using magnetic springs (magnets located at the ends to repel the free-sliding magnet) were presented. A first configuration having fixed magnets at the ends (top and bottom of the tubular structure) was placed in a backpack. It provided 0.3 mW when walking and 2.46 mW when slowly running. A second configuration with the top fixed magnet removed produced 0.95 mW when walking and 2.46 mW when slowly running. The second arrangement had a higher sliding magnet displacement for a 300% increase in power output while walking and 32% increase while slowly running. The energy stored in a $Li-MnO_2$ coin coil cell battery reached 3.5 J after 1 h of walking. The energy generated exceeded the power consumption of 700 μW (2.5 J in 1 h) for a wearable system composed of a light sensor, microphone, accelerometer, microprocessor, and RF transceiver.

Impact forces have also been studied for energy harvesting using piezoelectric materials. For example, a linear impact-based generator was proposed by Renaud et al. (2005) for harnessing limb motion. This design consisted on a free-sliding mass (750 mg) with piezoelectric cantilever beams at the ends for 10 mm displacement. When the sliding-mass impacts the cantilever beams, they resonate generating energy for an estimated power output of 40 μW. Further work (Renaud et al., 2009) tested a prototype (25 cm^3, 60 g sliding mass) that produced 47 μW

when turned over every second and generated 600 μW at 10 Hz for 10 cm linear displacement amplitude. A similar approach was also presented by Cavallier et al. (2005) but using tin balls and several PZT cantilever beams in a circular package (2 mm high, 14 mm diameter). In spite of the fact that the objective was to compare the efficiency of PZT cantilever beams versus stacks of PZT−Silicon−PZT, the study demonstrated the use of low frequencies to excite vibrations in structures at higher frequency without the need of frequency tuning. The evaluation of the prototype was performed using one element tested at a frequency of 6 Hz generating 62 nW. The complete generator with all the elements would generate around 0.5 μW.

Prosthetic knee implants is another area where piezoelectric generation has been studied, as evaluated by Platt et al. (2005a,b). Piezoelectric transduction benefits from the knee location because forces can be up to three times higher than the body weight. A laboratory test was elaborated using three piezoelectric stacks (1 cm × 1 cm × 2 cm). The prototype was capable of producing 850 μW of continuously regulated power (19% electrical efficiency, 20% electromechanical efficiency).

A muscle-powered piezoelectric generator was presented by Lewandowski et al. (2007). The generator was devised to be positioned in series with a muscle tendon to use the muscle contraction for piezoelectric stack compression. Power generation would benefit more from electrically stimulated muscle rather than natural muscle contractions. Hence, individuals with extensive paralysis are preferable, as electrically stimulated muscle would not interfere with natural muscle movement or other activities. In addition, the power needed to electrically stimulate the muscles is minimal in comparison with the power that a muscle can generate when using this generator. The forearm muscle (brachiocardialis), the dorso-lateral muscle on the trunk (latissimus dorsi), and the calf muscle (gastrocnemius) are capable of forces of 50, 100, and 250 N, respectively. These forces on a piezoelectric stack (5 mm × 5 mm cross-sectional area, 1 Hz, and 250 ms) can produce power outputs of 8 μW (2.5 cm long, at brachiocardialis), 54 μW (4 cm long, at latissimus dorsi), and 690 μW (8 cm long, at gastrocnemius). A PZT stack prototype (5 mm × 5 mm × 18 mm) produced up to 80 μW for a 250 N force. Muscle, tendon, and bone attachments were not mentioned in this investigation.

Tashiro et al. (2002) developed a variable-capacitance-type electrostatic generator for harnessing the ventricular wall motion of a dog's heart

using a honeycomb structure. The motion of the left ventricular wall was measured for testing a prototype resonating at 6 Hz. This prototype was made of stacked strips (50 layers, 20 cells per layer) of corrugated polyester film with evaporated aluminum (50 mm × 30 mm × 30 μm) and a mass (780 g) on top. An accelerometer placed on a dog's heart was used to drive a test setup with the same motion. The power output from the generator driven with the replicated heart motion was employed to pace the dog's heart at 180 bpm for over 2 h. An average of 36 μW power was obtained while for the stimulation pulse 18 μW was required.

Mitcheson et al. (2004a) reported an electrostatic nonresonant prototype employing a variable-gap parallel-plate capacitor. For a precharge of 30 V producing 0.3 μJ per cycle, 250 V were generated. This arrangement followed the coulomb-force parametric-generator (CFPG) architecture (using the contact force to damp the movement) described in Mitcheson et al. (2004b) and was reported as suitable for large amplitudes and low frequencies. Energy is produced only when the inertial force is larger than the damping force. A capacitor plate (200 mm^2) with a proof mass made of stacked silicon plates (10 mm × 11 mm × 0.4 mm) was fabricated for a maximum displacement of 450 μm. The final discharge of 250 V was produced by a capacitance change from 15 to 127 pF (11 pF parasitic capacitance). Other work from this group presented a modified version of this parallel-plate capacitor. Energy of 120 nJ and voltages up to 220 V were reported per cycle (using 30 V of charging voltage), although up to 2.6 μJ per cycle could be obtained for an optimized device (80 μW of power at 30 Hz). It is expected that if using gold as the proof mass material, the power output could be increased up to 10 times.

Arakawa et al. (2004) used an electret-based approach to avoid the need of precharging. An overlapped area capacitor using amorphous perfluoropolymer (CYTOP), as the electret, was presented. This electret material choice presented a charge density up to 0.68 mC/m^2 which produced 6 μW with a sinusoidal input oscillation of 1 mm at 10 Hz. Later work from this group was presented by Tsutsumino et al. (2006). They were able to reach a charge density as high as 1.37 mC/m^2 using corona discharging on a 15 μm film with 1,000 V of average surface voltage. At 20 Hz and 2 $mm_{p\text{-}p}$ vibration amplitude (150 V sinusoidal peak-to-peak waveform), 38 μW of power output was achieved. When compared against Teflon AF, CYTOP presents a surface charge density, σ, about 3× larger. A 9× increase in power generation could be

expected as power output is proportional to σ^2. The surface charge density was sustained for more than 100 days, and it was stable up to its glass transition temperature, $\sim 108^{\circ}$C. The capacitor plates consisted of rectangular areas (10 mm $\times$ 20 mm) covered with electrodes (1 mm wide, 30 μm gap) and separated by an air gap (100 μm). For a prototype having 200 μm wide electrodes (50 μm gaps) and oscillations of 1 $mm_{p\text{-}p}$ at 20 Hz, 1 mW of power can be generated.

Boland et al. (2005) used fixed electret plates with liquid droplets in between, called a liquid electret power generator (LEPG). The electret plates were covered with Teflon, and the dielectric was made of liquid droplets in addition to air. Polar liquids present high dielectric constants producing large capacitance changes when air is replaced by droplets. When the generator vibrates, the liquid droplets change the capacitance of this arrangement producing energy. The prototype was reported to produce 0.11 μW of power at 60 Hz, although it could produce up to 10 μW of power.

ZnO nanowires have also been suggested for energy generation (Liu et al., 2008; Wang, 2008; Wang et al., 2008). Gao et al. (2007) indicated that the use of flexible substrates would enable the use of piezoelectric nano arrays for bendable power sources in implantable biosensors. A single nanowire is known to generate 50 mV, thus arrays of nanowires could produce enough from energy harvesting. Such nano arrays have reported power densities of 100–200 $\mu W/cm^2$ (Gao et al., 2007). Power densities close to 83 nW/cm^2 for nanowires stimulated by ultrasonic waves have also been reported (Liu et al., 2008).

Energy generation has also used spherical geometries using electromagnetic transduction. Two devices having 1.5–4 cm^3 were presented by Bowers and Arnold (2008). The devices were held in the hand and a pocket during walking and running tests. Electrical power as high as 1.4 mW was reported. A planar rotational electromagnetic device was presented by Romero et al. (2011). The effective volume of the generator was reported as 2 cm^3. The device was capable of producing up to 427 μW of power while walking on a treadmill and up to 540 μW when running. This generator was evaluated at several body locations and different walking and running speeds.

Figures 3.1–3.3 summarize the findings of energy harvesters for body motion. Figure 3.1 shows a review of energy generators by the frequency of operation, whereas Figure 3.2 provides a representation

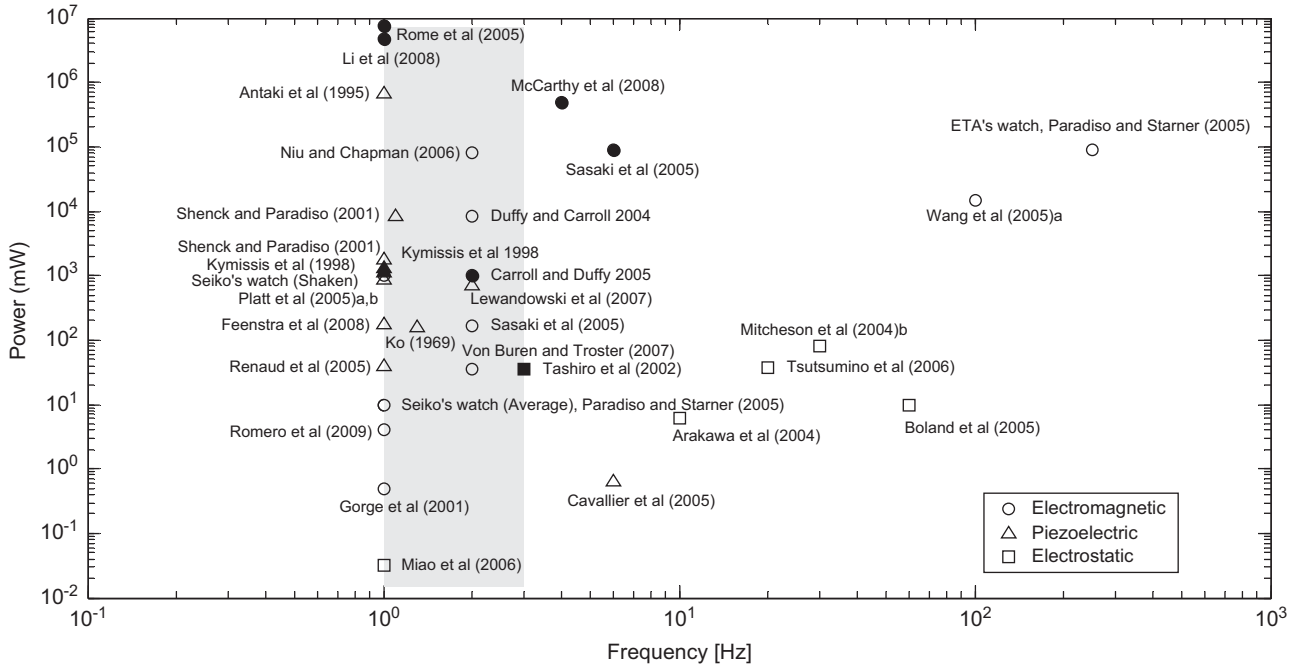

Figure 3.1 Summary of energy harvesters by frequency of operation. Shapes represent the transduction technology with the filled symbols for generators with volume greater than 10 cm^3 and the open symbols representing generators with volumes less than 10 cm^3. The shaded area represents frequencies associated with body motion from 1 to 3 Hz.

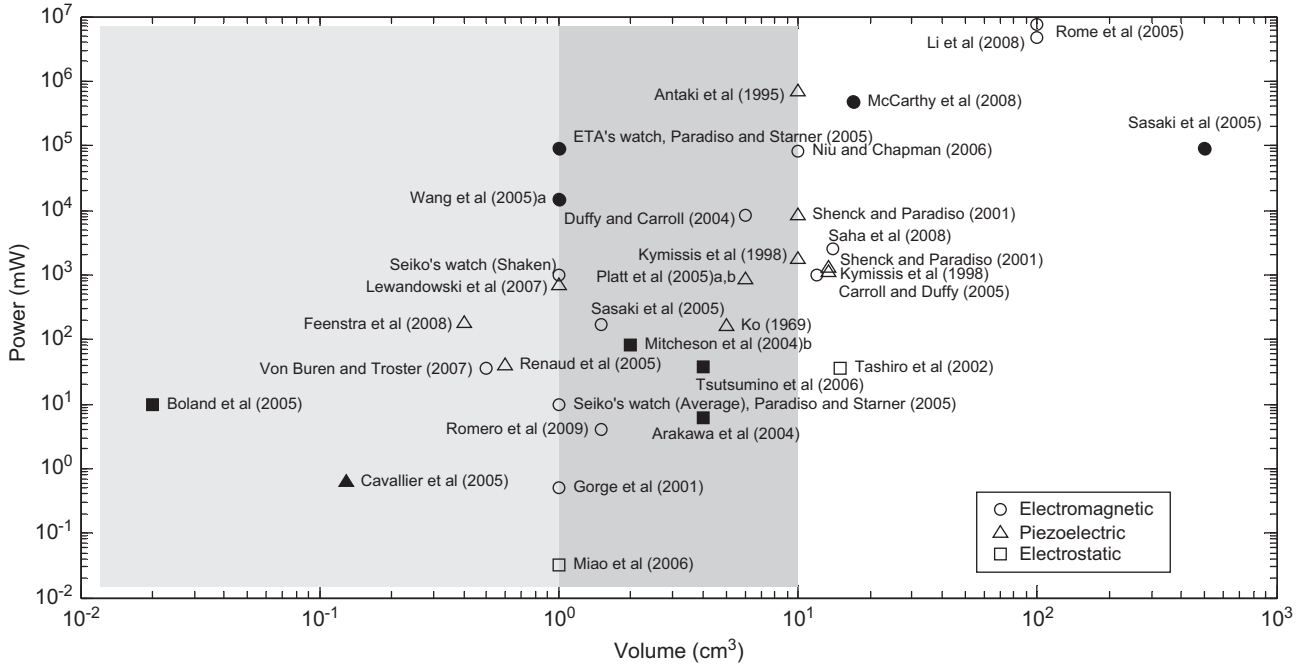

Figure 3.2 Summary of energy harvesters by generator's volume. Shapes represent the transduction technology with the filled symbols for generators with operating frequencies greater than 3 Hz and the open symbols representing generators operating at frequencies less than 3 Hz. The clear-shaded area represents volumes smaller than 1 cm^3, while the darker area is for volumes between 1 and 10 cm^3.

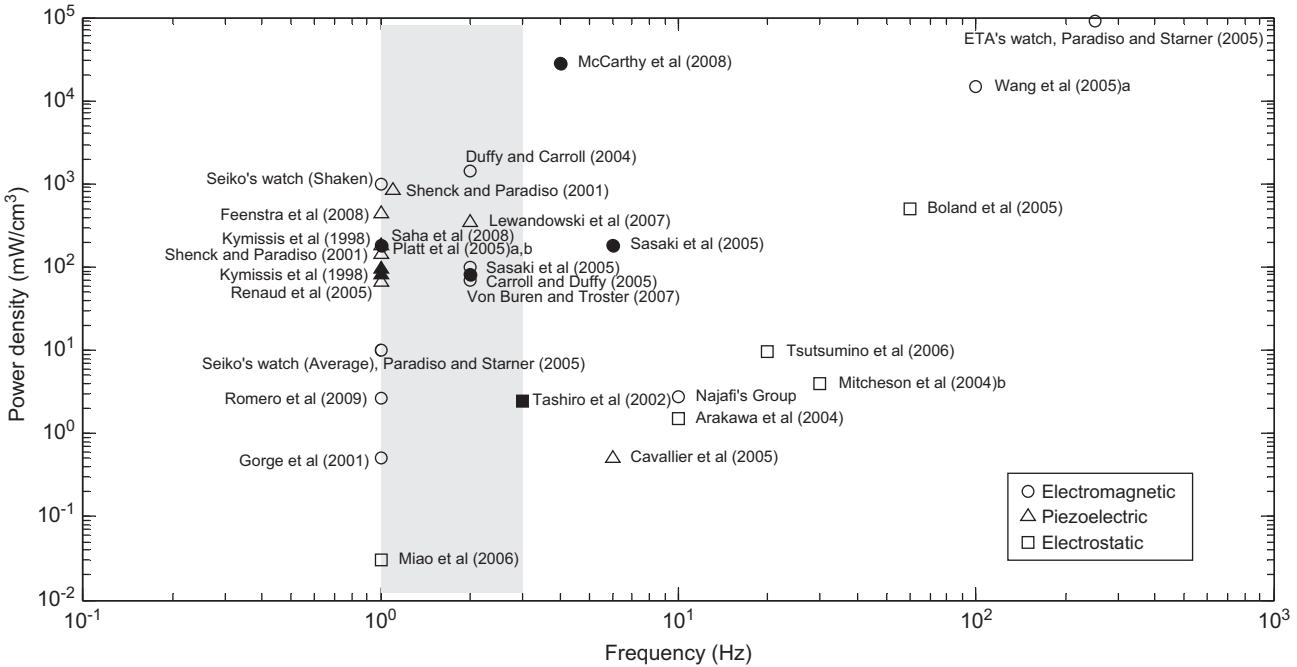

Figure 3.3 Summary of reported energy harvesters by power density. Shapes represent the transduction technology with the filled symbols for generators with volume greater than 10 cm^3 and the open symbols representing generators with volumes less than 10 cm^3. The shaded area represents frequencies associated with body motion from 1 to 3 Hz.

of the energy harvesters by volume. Figure 3.1 is mainly dominated by electromagnetic and piezoelectric transduction generators at frequencies close to 1 Hz, making them preferable over electrostatic generators. Filled symbols show the trend that larger devices are able to produce a higher power output. Devices operating at 1 Hz were reported to produce from less than 1 μW up to 7 W of power, at the expense of the generator's size. Figure 3.2 describes better this trend where larger devices were reported to produce a larger power. According to this chart, devices on the order of 1 cm^3 were reported to produce from less than 1 μW up to ~1 mW for generators operating at frequencies close to walking. Figure 3.3 summarizes that generators operating at 1 Hz presented power densities between ~1 $\mu W/cm^3$ and ~1 mW/cm^3.

The shaded area in Figure 3.1 represents the range of frequencies commonly associated with body motion activities. Those generators that are found inside this region are potential candidates for portable devices and/or biomedical applications. Although piezoelectric generators presented a relatively large power output, a percentage of them were designed to be placed inside shoes which might not be the most desirable location. The clear-shaded area in Figure 3.2 corresponds to the zone for miniature systems with energy harvesters smaller than 1 cm^3 (1 μW−1 mW power output). The designs from von Buren and Troster (2007) and Renaud et al. (2005) are suitable solutions for portable or implantable devices in that size range, although power output is below 50 μW, whereas the Feenstra et al. (2008) device produced a higher output but it is designed to be placed in backpack straps. The darker shaded region encompasses devices with volumes between 1 and 10 cm^3, which is populated with a larger variety of energy harvesters. Generators in this region can be selected according to the application constraints since power output goes from less than 1 μW to several milliwatts. Devices with volumes over 10 cm^3 seem to be more appropriate for portable or wearable systems because of the larger dimensions.

Figure 3.3 better describes the energy generation panorama for generators operating at frequencies between 1 and 3 Hz. The chart does not include all the reviewed generators because not all publications provided the power output or the device's volume to estimate the power density values. It can be appreciated that generators are capable of producing power densities as high as 1 mW/cm^3 for devices with a

volume smaller than 10 cm^3, while most devices were found in the range of 100−1,000 $\mu W/cm^3$. From this chart, most electrostatic energy harvesters were found to produce less than 100 $\mu W/cm^3$, making this transduction technique less competitive in comparison to electromagnetic or electrostatic generation. Therefore, the power density chart makes it easier to design systems for a given set of constraints.

From the charts, electromagnetic and piezoelectric generators were found to provide the largest amount of power per unit volume, with electromagnetic devices having a relatively higher output. Most of the evaluated harvesters were generators with linear displacement, whereas human motion is three-dimensional, presenting linear displacements and rotations. Thus, generator designs that harvest energy from more than one direction or that harness the joint rotations could be better suited for body motion. In this case, electromagnetic generation with rotational architectures could have an advantage over piezoelectric devices with linear designs. Only the impact-based piezoelectric design from Cavallier et al. (2005) takes advantage of a three-dimensional motion approach, but its power output was too low (less than 0.1 μW).

These charts can help to determine technologies and constraints for different applications. Although devices with volumes over 10 cm^3 can produce milliwatts of power, devices with dimensions on the order of 1 cm^3 present potential applications due to their reduced sizes for embedded or surgically implantable applications. Actual technology limits power output for the latter to hundreds of microwatts.

As summarized in Figure 3.3, electromagnetic generators with rotational designs were found to have high power densities (ETA's watch, Seiko's watch, Wang et al., 2005a) in small volumes (less than 10 cm^3). Because the size of generators can be reduced by means of MEMS technology, smaller energy harvesters for body motion can be fabricated with high power density using rotational electromagnetic generation.

CHAPTER 4

Power Consumption and Applications

Biomedical devices encompass a broad spectrum of applications; those that require power and those that not. These devices range from contact lenses, bone implants, stents, surgical instruments, cardiac pacemakers to blood glucose monitors. Powered biomedical equipment has relied on the power grid and/or batteries for operation due to the power requirement of devices. As medical technology evolved, devices decreased in size and became portable and even implantable such as pacemakers. Within implantable medical devices (IMDs), they can be divided into passive (structural devices) or active devices (powered devices). Table 4.1 provides a reference for the power requirements of several powered devices. At the same time, biomedical equipment has different power requirements.

There are new promising technologies for health-care monitoring: wireless body area networks and wireless personal area. Thus, actual power sources will be challenged even more with the increasing use of wireless communications. Wireless communications are still constrained with the unwieldy wires for tethered connections between the sensors and the central unit, and the implementation of energy-aware communication for wireless protocols (Jovanov et al., 2005). For example, the use of Bluetooth standard employing two AA batteries can function for 1–7 days (wake up time ~ 3 s, 700 kbps data rate, 7 nodes, 10 m range), while the use of the ZigBee wireless standard

Table 4.1 Orders of Magnitude of Power Requirements

Equipment	Power (W)
Powered exoskeleton	$\sim 10^{2}$
Powered prosthesis	~ 10
Retinal stimulator	$\sim 10^{-1}$
Neural recording	$\sim 10^{-2}$
Analog cochlear processor	$\sim 10^{-3}$
Hearing aid	$\sim 10^{-4}$
Pacemaker	$\sim 10^{-5}$
Wristwatch	$\sim 10^{-6}$

allows operation from 6 to 24 months using the same batteries (wake up time ~15 ms, 250 kpps data rate, 64,000 nodes, 30 m range), as pointed out by Hao and Foster (2008). Wired connections limits a broader deployment of sensors (mainly in remote locations and large physical areas), while wireless sensors are usually limited by lifespan and size (or weight) of batteries.

Electronic prostheses have batteries that need to be charged often because power consumption is quite high, in the order of 1 W. Batteries for powered prostheses have higher capacity as power consumption is higher. Batteries for IMDs account for 25–60% of the volume of implanted devices; this produces relatively large devices in order to last for several years (Schmidt and Skarstad, 2001). Batteries for pacemakers have an average duration of 5–12 years with power consumption that tops at 100 μW (Katz and Akiyama, 2007; Mallela et al., 2004; Schmidt and Skarstad, 2001). Implantable neurostimulators and infusion pumps have a lifespan of 3–5 years because of the higher power requirements (Paulo and Gaspar, 2010; Schmidt and Skarstad, 2001). Power consumption of hearing aids varies significantly depending on the model and capabilities of the device, power requirements vary from 50–2,000 μW. The small button cell used needs to be replaced periodically, as short as a few days in some cases (Flipsen et al., 2004). The main advantage of implantable devices with longer battery lifespan is the reduction in the surgeries for replacing batteries (and the device itself), which reduces health-care costs and enhances patient quality of life.

Nowadays there is a number of IMD in use to treat several conditions, from heart conditions (bradycardia, tachyarrhythmia, fibrillation), muscle stimulators (incontinence), neurological stimulators (deep brain, spinal cord), and cochlear implants to drug pumps (Soykan, 2002). Table 4.2 summarizes common IMD. Powering these devices has been

Table 4.2 Implantable Medical Devices

- Cardiac pacemakers
- Cardiac defibrillators
- Muscle stimulators
- Neurological stimulator
- Cochlear implants
- Monitoring devices
- Drug pumps

Table 4.3 Applications and Power Consumption

Application	IMD	Battery Chemistry	Power Requirements	Battery Duration
Bradycardia	Pacemaker	Li/I_2	30–100 μW	5–12 years
Tachycardia, fibrillation	Cardioverter defibrillator	Li/SVO, $Li/Ag_2V_4O_{11}$	30–100 μW (pacing) +10 W for defibrillation	4–7 years
Chronic pain, deep brain stimulation	Spinal cord stimulator (SCS); Deep brain stimulator (DBS)	$Li/SOCl_2$	300 μW to 50 mW	3–6 years
Bladder control	Sacral nerve stimulation (SNS)	Li/SVO, $Li/SOCl_2$	300 μW to 50 mW	3–5 years
Hearing loss	Cochlear Implant	Zinc-Air	200 μW to 5 mW	10–60 hours
Spasticity	Drug Pump	$Li/SOCl_2$	100 μW to 2 mW	4–8 years

Schmidt and Skarstad (2001)
Zeng et al. (2008)
my.clevelandclinic.org/services/sacral_nerve_stimulation/hic_sacral_nerve_stimulation.appx
www.medtronic.com/patients/parkinsons-disease/living-with/replacement/index.htm
www.neurosurgery.pitt.edu/imageguided/movement/stimulation.html
www.ncbi.nlm.nih.gov/pubmed/23367325
www.medgadget.com/2012/08/codmans-medstream-infusion-system-for-spinal-drug-deliver-gets-fda-ok.html
http://professional.medtronic.com/pt/neuro/itb/prod/synchromed-ii/index.htm

done through batteries or by external powering sources (radio frequency). Table 4.3 overviews the applications, power requirements, and service life for some of the IMDs.

Finally, Figure 4.1 makes a comparison of the power consumption of several biomedical devices against the power generation of reported energy harvesters in the literature. There are a number of generators that can be matched to medical applications. For instance, powered knee and leg prosthesis could use the knee-mounted brace (Li et al., 2008) or the backpack-generator (Rome et al., 2005). Cochlear implants and hearing aids could have thermal generators integrated into their designs for extended battery life. Hearing devices enjoy the possibility of thermal generator, because locations around the ear or head could use a large thermal gradient without clothing obstruction. Analyzing the plot, there are several approaches for powering cardiac pacemakers or similar power-budget devices. A number of the generators with relatively large power output were designed to harness energy while placed inside the shoes, which makes the integration with other devices challenging. From the summary figure, some electromagnetic prototypes, such as those presented by Bowers and Arnold (2008) and

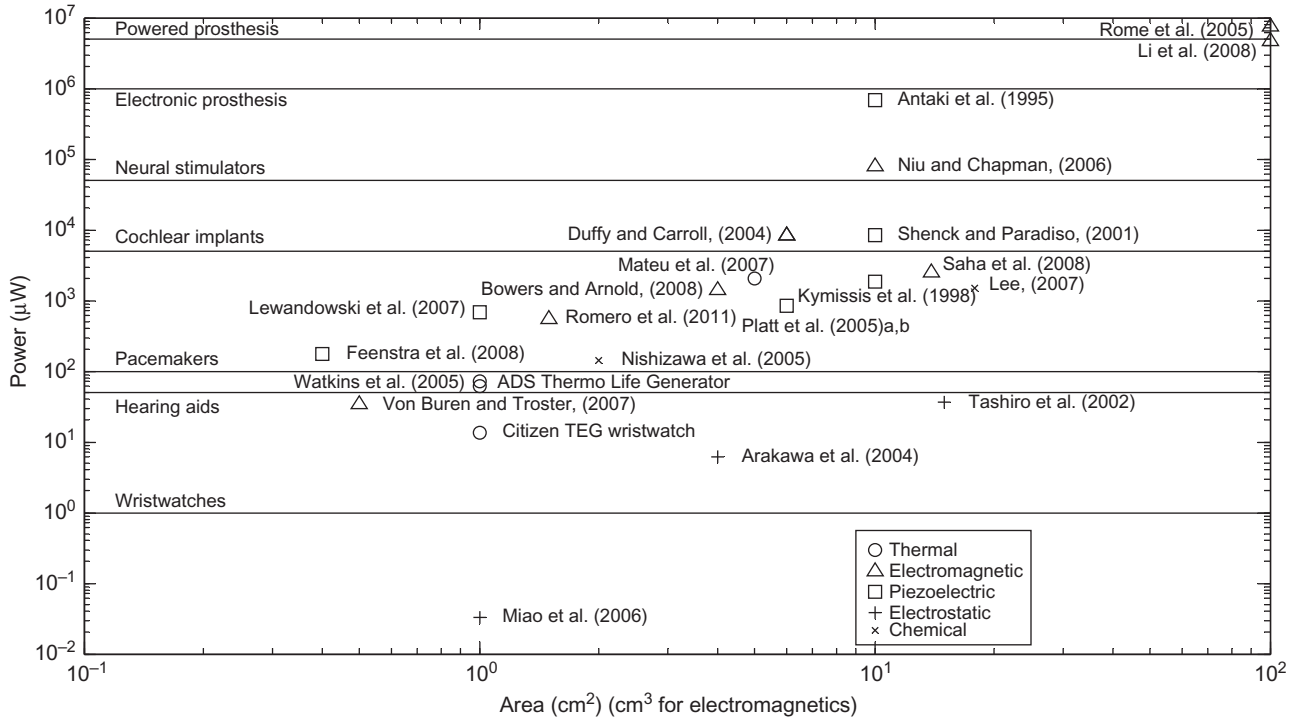

Figure 4.1 Power consumption of medical devices versus power generation of reported energy harvesters operating below 10 Hz. Wristwatches added for comparison purposes.

Romero et al. (2011), show promise for powering some IMDs. Considering an average volume of 20 mL (20 cm^3) for pacemakers, or a volume of about 10 cm^3 for the battery volume, there are also interesting options for small generators. Although this review has not found a large number of prototypes that could power some of the biomedical devices, it shows that this area is evolving rapidly compared to a decade ago.

Thus, the list should keep growing until more generators can satisfy the need of actual devices or new applications are developed around actual approaches. One interesting generator is the one presented by Platt et al. (2005a) for knee implants. One possible outcome for the Platt et al. (2005a) work is that in the near future, knee replacements could be instrumented to determine if misalignment happens at early stages. This way, knee-braces, physical therapy, or minor surgeries would eliminate some of the revision surgeries that are performed (Romero and Rincon, 2012). Many other new applications could also arise from today's passive biomedical devices to tomorrow's active monitoring devices, let it be for physiological responses or development. The future will tell.

CHAPTER 5

Future Trends

5.1 CHALLENGES

There are limitations that challenge energy scavenging at small scales such as the energy generation efficiency, energy density, rectification, energy storage and management, manufacturing, longevity, and packaging. A summary of these challenges is discussed to highlight some of the difficulties that need to be resolved in the near future for energy harvesting to be a practical energy source for portable, embedded, or implantable applications.

Energy generation from inertial approaches at smaller scales faces limitations due to the reduced mass sizes because power is directly proportional to mass. For example, a proof mass with a volume of 1 mm^3 has a maximum available power of 1 μW (volumetric power density of 1 mW/cm^3) for a generator attached to a walking person. Yet, only a few reported devices are close to that figure of the volumetric power density. Hence, generator size, placement, and power requirements must be evaluated. Parallel-plate electrostatic generators need to have air−gap displacements between 0.5 μm and hundreds of micrometers in order to generate power comparable to electromagnetic or piezoelectric devices, as estimated by Roundy (2005). This displacement range severely challenges the implementation and stability of electrostatic generators. Electrical generators usually are more efficient with increasing sizes, this means that efficiency does not scale well with smaller dimensions. Furthermore Roundy (2005) showed that electromagnetic, piezoelectric, and electrostatic generation have the possibility of high coupling coefficients (0.6−0.8). Therefore, the main challenge is to design miniature energy harvesters with efficiencies as high as the models predict. In addition, trying to recreate high efficiencies at smaller scales is a difficult task. Finding materials with the same properties as the bulk materials with tight tolerances and same reliability as the larger counterparts while being cost competitive is also difficult. Rectification is still the biggest obstacle because the threshold voltages represent a large fraction of the low voltages produced, and this

fraction of these voltages is lost. Electromagnetic generation is the king at the macroscale, at the MEMS-scale they are typically limited by the permanent magnet (PM) fabrication, as MEMS-compatible processes cannot replicate bulk PM material properties.

Linear generators with free-sliding masses and rotational devices are also limited by low-friction technology to minimize the mechanical damping, which is significant at smaller sizes. Rotational devices are the most susceptible as low-friction MEMS-based bearings are needed. Several new technologies are being developed to overcome this limitation: microball bearings (Ghalichechian et al., 2007, 2008; Waits et al., 2007), rotating pivots (Wang et al., 2005b), and magnetic bearings (Fernandez et al., 2000; Ghantasala et al., 2000). In addition, generators under vacuum present fewer losses due to air damping but create the need for special packaging. Packaging is also a constraint for devices operating in harsh conditions, such as bioimplanted applications. Fabrication techniques at the microscale are well established for piezoelectric and electrostatic generators because of the uncomplicated geometries they present. On the other hand, electromagnetic generators are limited by the availability of high-performance magnets and high-density coils at the microscale, although they are preferred for energy generation at larger sizes. Piezoelectric and electrostatic generators are also characterized by their relatively high voltages and low currents, whereas electromagnetic generators provide the opposite. Therefore, the selection of one of the transduction techniques is dependent on the energy source and the desired output characteristics for specific applications. Reliability is a point to consider because kinetic energy harvesters use moving parts (the rotor) and no long-term studies have been undertaken. Wristwatch technology can be employed as the mechanics of the generator are similar to those from the wristwatch industry. Although being relatively complex mechanical devices, wristwatches are considered a reliable and proven technology. Therefore, wristwatch bearing system assemblies might be used and adapted to rotational energy harvesters to improve reliability and performance.

The output for most energy harvesters is usually a time-variant AC signal; however, DC rectification and voltage regulation are needed to power most electronic circuits. The forward-bias voltage for diodes on bridge rectification circuits (>200 mV for Schottky diodes) can be high for the low-voltage generated from some devices. In these

cases, voltage multipliers have been employed to increase and rectify the output voltages. Some of the limitations faced by the use of semiconductor p−n junctions can be overcome by the use of active electronics (Amirtharajah et al., 2006; Makihara et al., 2006; Marzencki et al., 2008; Peters et al., 2008; Siebert et al., 2005).

Because the energy generation process from energy harvesting is heavily dependent on the availability of the external energy source, the produced energy must be stored for use when the energy source is unavailable. Capacitors and rechargeable batteries are the traditional energy storage elements that have been used for this purpose. Rechargeable batteries are preferable because of their high energy storage capacity, but they have a limited number of charging cycles. Capacitors can be charged quickly an infinite number of times, although the energy storage capacity is relatively low. On the other hand, electrochemical double-layer capacitors (supercapacitors or ultracapacitors) provide almost unlimited recharges with relatively high energy storage capacity. Supercapacitors with sizes resembling a postage stamp with capacities of 5−19 F have been presented (Flipsen, 2005; van Donk, 2000). Thin-film lithium batteries can also reduce the size of rechargeable power sources for biomedical applications (Albano et al., 2007; Bates et al., 2000; Bharatula et al., 2005; Harb et al., 2002). Studies reporting the successful use of rechargeable batteries using piezoelectric energy harvesters have also been carried out (Sodano et al., 2005a,b).

5.2 FUTURE

The increase in population ageing will take a toll on the developed economies. For sure, something will be done in order to minimize this impact. Better health-care monitoring (treating before it gets more complicated and/or expensive) as well as to keep the population more active will surely be one of the keys to attack this problem. As a whole, this panorama will be a priority, otherwise health care cost and economic development will be jeopardized. Thus, physiological measurement is a field that is likely to become more important in the near future.

Today the measurement of physiological parameters is something that can be done at home with ease (body weight, heart rate, blood pressure, blood glucose) with no medical supervision. Later on more

parameters will be measured with even more sophisticated equipment with little to no medical intervention. More healthy lifestyles are a consequence of being able to take control of our bodies.

Advanced wearable medical equipment is already being in use for patients worldwide for the administration of insulin with controlled dosage that depends on blood glucose levels. This makes a segment of population more active and in control. It is expected that this trend will be extended to several other conditions, for example spasticity and the implantable drug pump for this condition.

The future for powering biomedical devices looks bright. Because technology is always evolving to smaller sizes, and lower power consumption, the trend should apply to energy harvesters into smaller sizes but larger power generation. Even nanotechnology promises higher performance for lithium batteries. Advances using silicon nanowires have the potential to increase charge capacity to 4,200 mAh/g (Chan et al., 2008).

Technology is rapidly growing; this makes it a possibility of not relying exclusively on batteries for powering electronic equipment. Research and commercial devices show that this is possible.

REFERENCES

Adams, L., 1995. Lithium battery power sources for remote or portable sensor applications. Sensors, 80–81.

Albano, F., Chung, M., Blaauw, D., Sylvester, D., Wise, K., Sastry, A., 2007. Design of an implantable power supply for an intraocular sensor, using power (power optimization for wireless energy requirements). J. Power Sources 170 (1), 216–224.

Amirtharajah, R., Chandrakasan, A.P., 1998. Self-powered signal processing using vibration-based power generation. IEEE J. Solid-State Circuits 33 (5), 687–695.

Amirtharajah, R., Collier, J., Siebert, J., Zhou, B., Chandrakasan, A., 2005. DSPs for energy harvesting sensors: applications and architectures. IEEE Pervasive Comput. 4 (3), 72–79.

Amirtharajah, R., Wenck, J., Collier, J., Siebert, J., Zhou, B., 2006. Circuits for energy harvesting sensor signal processing. In: Design Automation Conference, DAC 2006, July 24–28, San Francisco, California, USA, pp. 639–644.

Antaki, J.F., Bertocci, G.E., Green, E.C., Nadeem, A., Rintoul, T., Kormos, R.L., et al., 1995. A gait-powered autologous battery charging system for artificial organs. ASAIO J. (American Society for Artificial Internal Organs) 41 (3):M588–95.

Arakawa, Y., Suzuki, Y., Kasagi, 2004. Micro seismic power generator using electret polymer film. In: Power MEMS 2004, November 28–30, Kyoto, Japan, pp. 187–190.

Arnold, D.P., 2007. Review of microscale magnetic power generation. IEEE Trans. Magn. 43 (11), 3940–3951.

Barton, S.C., Gallaway, J., Atanassov, P., 2004. Enzymatic biofuel cells for implantable and microscale devices. Chem. Rev., 4867–4886.

Bates, J.B., Dudney, N.J., Neudecker, B., Ueda, A., Evans, C.D., 2000. Thin-film lithium and lithium-ion batteries. Solid State Ionics 135 (1–4), 33–45.

Beeby, S.P., Tudor, M.J., White, N.M., 2006. Energy harvesting vibration sources for microsystems applications. Meas. Sci. Technol. 17 (12), R175–R195.

Bharatula, N.B., Zinniker, R., Troster, G., 2005. Hybrid micropower supply for wearable-pervasive sensor nodes. In: Ninth IEEE International Symposium on Wearable Computers (ISWC'05), 6–10 November, Galway, Ireland, pp. 196–197.

Boland, J.S., Messenger, J.D.M., Lo, K.W., Tai, Y.C., 2005. Arrayed liquid rotor electret power generator systems. In: Micro Electro Mechanical Systems, MEMS 2005, January 30–February 3, Miami, Florida, USA, pp. 618–621.

Bowers, B., Arnold, D., 2008. Spherical magnetic generators for bio-motional energy harvesting. PowerMEMS 2008, Nov. 9–12, Sendai, Japan, pp. 281–284.

Carroll, D., Duffy, M., 2005. Demonstration of wearable power generator. In: European Conference on Power Electronics and Applications, EPE 2005, 11–14 Sep., Dresden, Germany, 10 pp.

Cavallier, B., Berthelot, P., Nouira, H., Foltete, E., Hirsinger, L., Ballandras, S., 2005. Energy harvesting using vibrating structures excited by shock. In: IEEE Ultrasonics Symposium, 18–21 Sep., Rotterdam, The Netherlands, vol. 2, pp. 943–945.

Chan, C.K., Peng, H., Liu, G., McIlwrath, K., Zhan, X.F., Huggins, R.A., et al., 2008. High-performance lithium battery anodes using silicon nanowires. Nat. Nanotechnol. 3, 31–35.

Chen, K., Merritt, D.R., Howard, W.G., Schmidt, C.L., Skarstad, P.M., 2006. Hybrid cathode lithium batteries for implantable medical applications. J. Power Sources 162, 837–840.

Cook-Chennault, K.A., Thambi, N., Sastry, A.M., 2008. Powering MEMS portable devices—a review of non-regenerative and regenerative power supply systems with special emphasis on piezoelectric energy harvesting systems. Smart Mater. Struct. 17, 043001.

Day, L., McNeil, I., 1995. Biographical Dictionary of the History of Technology. Routledge, London.

Drews, J., Fehrmann, G., Staub, R., Wolf, R., 2001. Primary batteries for implantable pacemakers and defibrillators. J. Power Sources 97–98, 747–749.

Duffy, M., Carroll, D., 2004. Electromagnetic generators for power harvesting. In: Power Electronics Specialists Conference, PESC 04, June 20–26, Aachen, Germany, vol. 3, pp. 2075–2081.

El-Hami, M., Glynne-Jones, P., White, N.M., Hill, M., Beeby, S., James, E., et al., 2001. Design and fabrication of a new vibration-based electromechanical power generator. Sens. Actuators A Phys. 92 (1–3), 335–342.

Feenstra, J., Granstrom, J., Sodano, H., 2008. Energy harvesting through a back-pack employing a mechanically amplified piezoelectric stack. Mech. Syst. Signal Process. 22 (3), 721–734.

Fernandez, V., Fandino, J., Sauvey, C., Yonnet, J.P., Reyne, G., Cugat, O., 2000. A design methodology for permanent magnet microbearings. IEEE Trans. Magn. 36 (4), 1919–1922.

Flipsen, B., Bremer, A., Jansen, A., Veefkind, M., 2004. Towards a selection method for designing alternative energy systems in consumer products. In: Proceedings of the TMCE April 12–16, Lausanne, Switzerland, pp. 8.

Flipsen, S.F.J., 2006. Power sources compared: the ultimate truth? J. Power Sources 162 (2), 927–934.

Flipsen, S.P.J., 2005. Alternative Power Sources for Portables and Wearables. Part 1: Power Generation and Part 2: Energy Storage. Personal Energy Systems Programme. Delft University of Technology, Delft, The Netherlands.

Gage, G.J., Ludwig, K.A., Otto, K.J., Ionides, E.L., Kipke, D.R., 2005. Naive coadaptive cortical control. J. Neural Eng. 2 (2), 52–63.

Gao, P.X., Song, J., Liu, J., Wang, Z.L., 2007. Nanowire piezoelectric nanogenerators on plastic substrates as flexible power sources for nanodevices. Adv. Mater. 19 (1), 67–72.

Gavrilov, L.A., Heuveline, P., 2003. Aging of population. In: Demeny, P., McNicoll, G. (Eds.), The Encyclopedia of Population. Macmillan Reference, New York, pp. 32–37.

Ghalichechian, N., Modafe, A., Beyaz, M.I., Ghodssi, R., 2007. A rotary micro-motor supported on microball bearings. In: Solid-State Sensors, Actuators and Microsystems Conference, Transducer 2007, June 10–14, Lyon, France, pp. 1123–1126.

Ghalichechian, N., Mccarthy, M., Beyaz, M.I., Ghodssi, R., 2008. Measurement and modeling of friction in linear and rotary micromotors supported on microball bearings. In: Micro Electro Mechanical Systems, MEMS 2008, Nov. 9–12, Sendai, Japan, pp. 507–510.

Ghantasala, M.K., Qin, L., Sood, D.K., Zmood, R.B., 2000. Design and fabrication of a micro magnetic bearing. Smart Mater. Struct. 9, 235–240.

Gorge, G., Kirstein, M., Erbel, R., 2001. Microgenerators for energy autarkic pacemakers and defibrillators: fact or fiction? Herz 26 (1), 64–68.

Goto, H., Sugiura, T., Kazui, T., 1998. Feasibility of the automatic generating system (AGS) for quartz watches as a leadless pacemaker power source: a preliminary report. In: Proceedings of Engineering in Medicine and Biology Society, Oct. 29–Nov. 1, Hong Kong, vol. 1, pp. 417–419.

Goto, H., Sugiura, T., Harada, Y., Kazui, T., 1999. Feasibility of using the automatic generating system for quartz watches as a leadless pacemaker power source. Med. Biol. Eng. Comput. 37 (1), 377–380.

Hao, Y., Foster, R., 2008. Wireless body sensor networks for health-monitoring applications. Physiol. Meas. 29, R27–R56.

Harb, J., Lafollette, R.M., Selfridgec, R.H., Howell, L.L., 2002. Microbatteries for self-sustained hybridmicropower supplies. J. Power Sources 104 (1), 46–51.

Hirasaki, E., Moore, S.T., Raphan, T., Cohen, B., 1999. Effects of walking velocity on vertical head and body movements during locomotion. Exp. Brain Res. 127 (2), 117–130.

Holmes, F.F., 2001. The role of lithium batteries in modern health care. J. Power Sources 97–98, 739–741.

Jansen, A.J., Stevels, A.L.N., 1999. Human power, a sustainable option for electronics. In: Electronics and the Environment, ISEE 1999, May 11–13, Danvers, Massachusetts, pp. 215–218.

Johnson, M.D., Otto, K.J., Williams, J.C., Kipke, D.R., 2004. Bias voltages at microelectrodes change neural interface properties in vivo. In: Engineering in Medicine and Biology Society, 2004. IEMBS '04. 26th Annual International Conference of the IEEE, Sep. 1–5, San Francisco, California, USA, vol. 2, pp. 4103–4106.

Jovanov, E., Milenkovic, A., Otto, C., Groen, P.C., 2005. A wireless body area network of intelligent motion sensors for computer assisted physical rehabilitation. J. Neuroeng. Rehabil. 2, 1–6.

Katz, D., Akiyama, T., 2007. Pacemaker longevity: the world's longest-lasting pacemaker. Ann. Noninvasive Electrocardiol. 12, 223–226.

Knoblauch, R.L., Pietrucha, M.T., Nitzburg, M., 1996. Field studies of pedestrian walking speed and start-up time. Transportation Research Record No. 1538, pp. 27–38.

Ko, W. H., 1969. Piezoelectric energy converter for electronic implants, U.S. Patent 3,456,134.

Kymissis, J., Kendall, C., Paradiso, J., Gershenfeld, N., 1998. Parasitic power harvesting in shoes. In: Wearable Computers, Oct. 19–20, Cambridge, Massachusetts, USA, pp. 132–139.

Lee, K.B., 2005. Urine-activated paper batteries for biosystems. J. Micromech. Microeng. 15, S210–S214.

Lewandowski, B.E., Kilgore, K.L., Gustafson, K.J., 2007. Design considerations for an implantable, muscle powered piezoelectric system for generating electrical power. Ann. Biomed. Eng. 35 (4), 631–641.

Li, Q., Naing, V., Hoffer, J.A., Weber, D.J., Kuo, A.D., Donelan, J.M., 2008. Biomechanical energy harvesting: apparatus and method. In: Robotics and Automation, 2008. ICRA 2008, May 19–23, Pasadena, California, USA, pp. 3672–3677.

Liu, J., Fei, P., Zhou, J., Tummala, R., Wang, Z.L., 2008. Toward high output-power nanogenerator. Appl. Phys. Lett. 92 (17).

Luchakov, Y.I., Nozdrachev, A.D., 2009. Mechanism of heat transfer in different regions of human body. Hum. Anim. Physiol. 36 (1), 53–57.

Makihara, K., Onoda, J., Miyakawa, T., 2006. Low energy dissipation electric circuit for energy harvesting. Smart Mater. Struct. 15 (5), 1493–1498.

Mallela, V.S., Ilankumaran, V., Rao, N.S., 2004. Trends in cardiac pacemaker batteries. Indian Pacing Electrophysiol. J. 4 (4), 201–212.

Maluf, N., Williams, K., 2004. An Introduction to Microelectromechanical Systems Engineering. Artech-House.

Marzencki, M., Ammar, Y., Basrour, S., 2008. Integrated power harvesting system including a mems generator and a power management circuit. Sens. Actuators A Phys. 145–46, 363–370.

Mason, A., Yazdi, N., Chavan, A.V., Najafi, K., Wise, K.D., 1998. A generic multielement microsystem for portable wireless applications. IEEE Proc. 86 (8), 1733–1746.

Mateu, L., Codrea, C., Lucas, N., Pollak, M., Spies, P., 2007. Human body energy harvesting thermogenerator for sensing applications. SENSORCOMM 2007, Oct. 14–20, Valencia, Spain, pp. 366–372.

Mccarthy, K., Bash, M., Pekarek, S., 2008. Design of an air-core linear generator drive for energy harvest applications. In Applied Power Electronics Conference and Exposition. APEC, 2008, pp. 1832–1838.

Miao, P., Mitcheson, P.D., Holmes, A.S., Yeatman, E.M., Green, T.C., Stark, B.H., 2006. Mems inertial power generators for biomedical applications. Microsyst. Technol. 12 (10), 1079–1083.

Minteer, S.D., Liaw, B.Y., Cooney, M.J., 2007. Enzyme-base biofuel cells. Curr. Opin. Biotechnol. 18, 228–234.

Mitcheson, P.D., Miao, P., Stark, B.H., Yeatman, E.M., Holmes, E.S., Green, T.C., 2004a. MEMS electrostatic micropower generator for low frequency operation. Sens. Actuators A Phys. 115 (2–3), 523–529.

Mitcheson, P.D., Green, T.C., Yeatman, E.M., Holmes, A.S., 2004b. Architectures for vibration-driven micropower generators. J. Microelectromech. Syst. 13 (3), 429–440.

Najafi, K., 2000. Low-power micromachined microsystems (invited talk). In: ISLPED '00, July 25–27, Rapallo, Italy, pp. 1–8.

Nishizawa, M., Togo, M., Takamura, A., Asai, T., Abe, T., 2005. Enzyme-based fuel cells from biomedical microdevices. In: PowerMEMS 2005, January 30–February 3, Miami, Florida, USA, pp. 177–181.

Niu, P., Chapman, P., 2006. Design and performance of linear biomechanical energy conversion devices. In: Power Electronics Specialists Conference, PESC '06, June 18–22, Jeju, South Korea, pp. 1–6.

Oweiss, K., Suhail, Y., Thomson, K., Li, J., Mason, A., 2005. Augmenting real-time DSP in implantable high-density neuroprosthetic devices. In: Third IEEE/EMBS Special Topic Conference on Microtechnology in Medicine and Biology, May 12–15, Kahuku, Oahu, Hawaii, USA, pp. 108–111.

Paradiso, J., Feldmeier, M., 2001. A compact, wireless, self-powered pushbutton controller. In: Ubicomp 2001: Ubiquitous Computing, Sep. 30–Oct. 2, Atlanta, Georgia, USA, pp. 299–304.

Paradiso, J.A., Starner, T., 2005. Energy scavenging for mobile and wireless electronics. IEEE Pervasive Comput. 4 (1), 18–27.

Paulo, J., Gaspar, P.D., 2010. Review and future trend of energy harvesting methods for portable medical devices. In: Proceedings of the World Congress on Engineering, WCE 2010 June 30–July 2, London, UK.

Paulo, J., Gaspar, P.D., 2010. Review and future trend of energy harvesting methods for portable medical devices. Lect. Notes Eng. Comput. Sci. 2184 (1), 909–914.

Peters, C., Spreemann, D., Ortmanns, M., Manoli, Y., 2008. A CMOS integrated voltage and power efficient AC/DC converter for energy harvesting applications. J. Micromech. Microeng. 18 (10), 104005.

Platt, S.R., Farritor, S., Garvin, K., Haider, H., 2005a. The use of piezoelectric ceramics for electric power generation within orthopedic implants. IEEE/ASME Trans. Mechatron. 10 (4), 455–461.

Platt, S.R., Farritor, S., Haider, H., 2005b. On low-frequency electric power generation with PZT ceramics. IEEE/ASME Trans. Mechatron. 10 (2), 240–252.

Rao, S.S., 1995. Mechanical Vibrations. 3rd ed, Englewood Cliffs, NJ: Prentice Hall.

Renaud, M., Sterken, T., Fiorini, P., Puers, R., Baert, K., van Hoof, C., 2005. Scavenging energy from human body: design of a piezoelectric transducer. In: Digest of Technical Papers. TRANSDUCERS '05, vol. 1, pp. 784–787.

Renaud, M., Fiorini, P., van Schaijk, R., van Hoof, C., 2009. Harvesting energy from the motion of human limbs: the design and analysis of an impact-based piezoelectric generator. Smart Mater. Struct. 18 (035001), 16.

Ritter, T., Geng, X., Shung, K.K., Lopath, P.D., Park, S.E., Shrout, T.R., 2000. Shrout.Single crystal PZN/PT-polymer composites for ultrasound transducer applications. IEEE Trans. Ultrason. Ferroelectr. Freq. Control 47 (4), 792–800.

Rome, L.C., Flynn, L., Goldman, E.M., Yoo, T.D., 2005. Generating electricity while walking with loads. Science 309 (5741), 1725–1728.

Romero, E., 2010. Energy Harvesting from Body Motion using Rotational Micro-Generation. PhD Dissertation, Michigan Technological University.

Romero, E., Neuman, M., Warrington, R., 2011. Rotational enegy harvester for body motion. MEMS, 2011, January 23–27, Cancun, Mexico, pp. 1325–1328.

Romero, E., Rincon, A., 2012. Piezoelectric load measurement model in knee implants. In: Proceedings of the EMBS 2012, Aug. 28–Sep. 1, San Diego, California, USA, pp. 511–514.

Romero, E., Warrington, R.O., Neuman, M.R., 2009. Energy scavenging sources for biomedical sensors. Physiol. Meas. 30, R35–R62.

Roundy, S., 2005. On the effectiveness of vibration-based energy harvesting. J. Intell. Mater. Syst. Struct. 16 (10), 809–823.

Roundy, S., Wright, P.K., 2004. A piezoelectric vibration based generator for wireless electronics. Smart Mater. Struct. 13 (5), 1131–1142.

Roundy, S.J., 2003. Energy Scavenging for Wireless Sensor Nodes with a Focus on Vibration to Electricity Conversion. PhD thesis, University of California, Berkeley.

Saha, C.R., O'Donnell, T., Wang, N., Mccloskey, P., 2008. Electromagnetic generator for harvesting energy from human motion. Sens. Actuators A Phys. 147 (1), 248–253.

Sasaki, K., Osaki, Y., Okazaki, J., Hosaka, H., Itao, K., 2005. Vibration-based automatic power-generation system. Microsyst. Technol. 11 (8), 965–969.

Schroeppel, E. A., 1987. Pacing lead with piezoelectric power generating means, U.S. Patent 4,690,143.

Seok, M., Hanson, S., Lin, Y.S., Foo, Z., Kim, D., Lee, Y., et al., 2008. The phoenix processor: a 30 pw platform for sensor applications. In: IEEE Symposium on VLSI Circuits, June 18–19, Honolulu, Hawaii, USA, pp. 188–189.

Schmidt, C.L., Skarstad, P.M., 2001. The future of lithium and lithium-ion batteries in implantable medical devices. J. Power Sources 97–98, 742–746.

Shenck, N.S., Paradiso, J.A., 2001. Energy scavenging with shoe-mounted piezo-electrics. IEEE Micro 21 (3), 30–42.

Siebert, J., Collier, J., Amirtharajah, R., 2005. Self-timed circuits for energy harvesting AC power supplies. In: Low Power Electronics and Design, ISLPED '05, Aug. 8–10, San Diego, California, USA, pp. 315–318.

Slob, P., 2000. The Human Power Chart Sustained Comfortable Cranking. PhD thesis, Delft University of Technology.

Sodano, H.A., Inman, D.J., Park, G., 2005a. Generation and storage of electricity from power harvesting devices. J. Intell. Mater. Syst. Struct. 16 (1), 67–75.

Sodano, H.A., Inman, D.J., Park, G., 2005b. Comparison of piezoelectric energy harvesting devices for recharging batteries. J. Intell. Mater. Syst. Struct. 16 (10), 799–807.

Soykan, O., 2002. Power sources for implantable medical devices. Med. Device Manuf. Technol., 76–79.

Starner, T., 1996. Human-powered wearable computing. IBM Syst. J. 35 (3–4), 618–629.

Starner, T., Paradiso, J.A., 2004. Human generated power for mobile electronics. In: Piguet, C. (ed.), Low Power Electronics Design, Chapter 45. CRC Press pp. 1–35.

Stephen, N.G., 2006. On energy harvesting from ambient vibration. J. Sound Vib. 293 (1–2), 409–425.

Tashiro, R., Kabei, N., Katayama, K., Tsuboi, E., Tsuchiya, K., 2002. Development of an electrostatic generator for a cardiac pacemaker that harnesses the ventricular wall motion. J. Artif. Organs 5 (4), 0239–0245.

Taylor, G.W., Burns, J.R., Kammann, S.A., Powers, W.B., Welsh, T.R., 2001. The energy harvesting eel: a small subsurface ocean/river power generator. IEEE J. Oceanic Eng. 26 (4), 539–547.

Tsutsumino, T., Suzuki, Y., Kasagi, N., Sakane, Y., 2006. Seismic power generator using high-performance polymer electret. In: Micro Electro Mechanical Systems, MEMS 2006, Jan. 22–26, Istambul, Turkey, pp. 98–101.

Van Donk, R.H., 2000. Design of an Alternatively Powered Remote Control. Master's thesis, Delf University of Technology.

Varshney, U., 2007. Pervasive healthcare and wireless health monitoring. Mobile Net-Works Appl. 12 (2–3), 113–127.

Von Buren, T., Troster, G., 2007. Design and optimization of a linear vibration-driven electromagnetic micro-power generator. Sens. Actuators A Phys. 135 (2), 765–775.

Waits, M.C., Geil, B., Ghodssi, R., 2007. Encapsulated ball bearings for rotary micro machines. J. Micromech. Microeng. 17 (9), S224–S229.

Wang, J., Wang, W., Jewell, G.W., Howe, D., 2005a. Design of a miniature permanent-magnet generator and energy storage system. IEEE Trans. Ind. Electron. 52 (5), 1383–1390.

Wang, R.R.J., Kamper, M.J., Van derWesthuizen, K., Gieras, J.F., 2005b. Optimal design of a coreless stator axial flux permanent-magnet generator. IEEE Trans. Magn. 41 (1), 55–64.

Wang, Z.L., 2008. Self-powered nanotech. Sci. Am. 298, 82–87.

Wang, Z.L., Wang, X., Song, J., Liu, J., Gao, Y., 2008. Piezoelectric nanogenerators for self-powered nanodevices. IEEE Pervasive Comput. 7 (1), 49–55.

Watkins, C., Shen, B., Venkatasubramanian, R., 2005. Low-grade-heat energy harvesting using superlattice thermoelectrics for applications in implantable medical devices and sensors. ICT2005, June 19–23, Clemson University, USA, 265–267.

Yang, R., Quin, Y., Li, C., Zhu, G., Wang, Z., 2009. Converting biomechanical energy into electricity by a muscle-movement driven nanogenerator. NanoLett 9 (3), 1201–1205.

Yazdi, N., Mason, A., Najafi, K., Wise, K.D., 2000. A generic interface chip for capacitive sensors in low-power multi-parameter microsystems. Sens. Actuators A Phys. 84 (3), 351–361.

Yeatman, E.M., 2008. Energy harvesting from motion using rotating and gyroscopic proof masses. Proceedings of the Institution of Mechanical Engineers, Part C: Journal of Mechanical Engineering Science, vol. 222, N. 1 pp. 27–36 doi: 10.1243/09544062JMES701.

Yeatman, E.M., Mitcheson, P.D., Holmes, A.S., 2007. Micro-engineered devices for motion energy harvesting. In: Electron Devices Meeting, IEDM 2007, Dec. 10–12, Washington DC, USA, pp. 375–378.

Zeng, F.G., Rebscher, S., Harrison, W., Sun, X., Feng, H., 2008. Cochlear implants: system design, integration, and evaluation. IEEE Rev. Biomed. Eng. 1, 115–142.